

A unifying view of gamma-ray burst afterglows

G. Ghisellini,^{1*} M. Nardini,² G. Ghirlanda¹ and A. Celotti²

¹INAF – Osservatorio Astronomico di Brera, Via Bianchi 46 I-23806 Merate, Italy

²SISSA – Via Beirut 2/4, I-34014 Trieste, Italy

Accepted 2008 November 6. Received 2008 November 6; in original form 2008 September 20

ABSTRACT

We selected a sample of 33 gamma-ray bursts detected by *Swift*, with known redshift and optical extinction at the host frame. For these, we constructed the de-absorbed and *K*-corrected X-ray and optical rest-frame light curves. These are modelled as the sum of two components: emission from the forward shock due to the interaction of a fireball with the circumburst medium and an additional component, treated in a completely phenomenological way. The latter can be identified, among other possibilities, as a ‘late prompt’ emission produced by a long-lived central engine with mechanisms similar to those responsible for the production of the ‘standard’ early prompt radiation. Apart from flares or re-brightenings, that we do not model, we find a good agreement with the data, despite of their complexity and diversity. Although based, in part, on a phenomenological model with a relatively large number of free parameters, we believe that our findings are a first step towards the construction of a more physical scenario. Our approach allows us to interpret the behaviour of the optical and X-ray afterglows in a coherent way, by a relatively simple scenario. Within this context, it is possible to explain why sometimes no jet break is observed; why, even if a jet break is observed, it is often chromatic and why the steepening after the jet break time is often shallower than predicted. Finally, the decay slope of the late prompt emission after the shallow phase is found to be remarkably similar to the time profile expected by the accretion rate of fall-back material (i.e. $\propto t^{-5/3}$), suggesting that this can be the reason why the central engine can be active for a long time.

Key words: radiation mechanisms: non-thermal – gamma-rays: bursts – X-rays: general.

1 INTRODUCTION

The gamma-ray burst (GRB) X-ray light curves, as observed by *Swift*, have shown a complexity unforeseen before. Besides the behaviour as observed by *BeppoSAX* after several hours from the trigger, a significant fraction of GRBs shows a steep flux decay soon after the end of the prompt as seen by the Burst Alert Telescope (BAT), followed by a plateau lasting for a few thousands seconds, ending at the time T_A (following Willingale et al. 2007). This trend, named ‘steep-flat-steep’ (Tagliaferri et al. 2005; Nousek et al. 2006), has been interpreted in several ways (for a recent review see e.g. Zhang 2007). Furthermore, in nearly half of the bursts, X-ray flares, of relatively short duration Δt , i.e. $\Delta t/t \sim 0.1$ (e.g. Chincarini et al. 2007), are observed even several hours after the trigger. Considering X-ray flares in different GRBs, Lazzati, Perna & Begelman (2008) have shown that their average luminosity decays as $t^{-5/3}$, similarly to what predicted following the mass accretion rate of fall-back material (see Chevalier 1989; Zhang, Woosley & Heger 2007).

The optical light curves are also complex, but rarely track the X-ray flux behaviour (see e.g. Panaitescu et al. 2006; Panaitescu 2007a,b), suggesting a possible different origin.

For 10–15 per cent of bursts, precursor emission is detected, preceding the main event in some cases by hundreds of seconds. The energy contained in the precursors is comparable to that in the main event, and the spectra in the two phases are indistinguishable (Burlon et al. 2008), suggesting that they are produced by the same mechanism.

Much theoretical effort has been made to understand the ‘steep-flat-steep’ behaviour, shown especially by the X-ray light curve. The initial steep decay is interpreted as ‘curvature’ (or ‘high latitude’) emission of the fireball: when the prompt ceases, the emission is dominated by radiation produced from parts of the fireball not exactly pointing at us (Nousek et al. 2006; Zhang et al. 2006, but see e.g. Pe’er, Mészáros & Rees 2006 for an alternative interpretation). At later times, the relatively steep decay observed after T_A is generally explained as the ‘standard’ forward (external) shock emission, namely as corresponding to the X-ray afterglow phase typically observed by *BeppoSAX* several hours after the burst trigger. There are, however, some alternative interpretations (see below). The most

*E-mail: gabriele.ghisellini@brera.inaf.it

puzzling phase is the shallow, or plateau, one. Several models have been proposed, aiming at accounting not only for the shallow flux decay but also why it steepens at the break time T_A . The proposed alternative interpretations include the following.

(i) Energy injection. Zhang et al. (2006) propose that the shallow decay can be produced by a continuous, long lasting, energy injection into the forward external shock. There are at least two possibilities, depending on whether the central engine is long or short lived. A long-lived engine could have luminosity that smoothly decreases as $L(t) \propto t^{-q}$ with $q < 1$ (Zhang & Mészáros 2001; Zhang et al. 2006), with T_A corresponding to the end of the energy injection phase.

A short-lived engine (i.e. of duration comparable to that of the prompt phase) can produce shells with a steep power-law distribution of Γ factors. T_A is determined by a cut-off in the Lorentz factor distribution. The two alternatives cannot be currently distinguished observationally. Both interpret the plateau as afterglow emission from a continuously refreshed shock. The required energetic (in bulk motion) largely exceeds what required to produce the prompt emission.

(ii) Reverse shocks. The shallow decay could be produced as synchrotron emission from the reverse external shock if the microphysical parameters ϵ_e and ϵ_B are much larger than those in the forward shock. In this situation, the ratio of the X-ray flux produced by the reverse and forward shocks would be dominated by the former. Along these lines, Uhm & Beloborodov (2007) and Genet, Daigne & Mochkovitch (2007) suggested that the X-ray plateau emission is due to the reverse shock running into ejecta of relatively small (and decreasing) Lorentz factors. This requires an appropriate Γ distribution of the ejecta, besides the suppression of the X-ray flux produced by the forward shock.

(iii) Time-dependent microphysical parameters. If the relativistic electron distribution has a typical slope $p \sim 2$, the X-ray luminosity is proportional to the bolometric luminosity ($L_X = \epsilon_e L_{\text{bol}}$). Since $L_{\text{bol}} \propto t^{-1}$, a time evolution of $\epsilon_e \propto t^{1/2}$ would produce $L_X \propto t^{-1/2}$, close to the observed plateau slopes. T_A is identified with the time ϵ_e reaches its maximum value (~ 0.1) (Ioka et al. 2006).

(iv) Precursor fireball (Ioka et al. 2006). In this scenario, a precursor, occurring 10^3 – 10^6 s before the main burst, generates a first fireball with low Γ , whose afterglow is too faint to be detected. The main burst then generates another, more powerful, fireball with a larger Γ . This second fireball, interacting with the first one, produces the plateau phase. When the two fireballs merge and interact with the circumburst medium, the standard afterglow sets in.

(v) Up-scattering of forward shock photons. Panaitescu (2008) suggested that a relativistic shell would scatter protons produced by a forward shock located ahead of it. While this occurs also if the relativistic shell does not dissipate (bulk Compton), the process is more effective if dissipation (through, e.g. internal shocks) occurs, heating the electrons of the shell. The up-scattered component is expected to be more relevant in X-rays than in optical, thus overshining the standard afterglow (i.e. forward shock) more easily in the X-ray band.

(vi) Geometrical models. If two co-aligned jets, with different opening angles, are observed at an angle θ_v within the wide cone, but outside the narrow one, the emission from the narrow jet would be visible only once it has decelerated. The observed light curve of the afterglow of the narrow jet would be flat before T_A , mimicking the observed plateau (see e.g. Racusin et al. 2008 for the case of GRB 080319B). In this model, the time T_A is the time at which the Lorentz factor Γ of the narrow jet decreases to $\sim 1/\theta_v$.

A somewhat similar model is the off-beam model by Eichler & Granot (2006) in which the shallow phase represents the smooth peak of an afterglow observed off-axis. Here too, T_A is identified by the time when the whole jet emission becomes visible.

In the patchy shell model, Toma et al. (2006) propose that the early X-ray afterglow could be produced by an inhomogeneous jet of aperture angle ~ 0.1 rad composed by multiple subjets subtending a smaller aperture ($\theta_{s-j} < 0.01$ rad). The latter ones are observable when their Γ decelerate to $\sim 1/\theta_v$. A shallow phase is ascribed to the superposition of the single subjet emissions, seen by an observer not exactly on-axis with any of them. When they merge due to sideways expansion, the normal afterglow begins to dominate: this corresponds to the time T_A . Therefore, the duration of the shallow phase depends on the (still uncertain) sideways expansion velocity.

(vii) Dust scattering. Shao & Dai (2007) interpret the plateau as prompt X-ray flux scattered by dust grains located in the burst surroundings (within ~ 100 pc). This model has been recently questioned by Shao, Dai & Mirabal (2008) as it predicts a strong spectral softening during the shallow decay phase, inconsistent with the data. Moreover, the large amount of the dust required would imply an optical extinction in excess of what observed.

(viii) Cannonballs. Dado, Dar & De Rújula (2005) propose that the entire steep-flat-steep behaviour of the X-ray light curve is due the sum of thermal bremsstrahlung and synchrotron emission from a cannonball decelerating in the circumburst medium. The time T_A would correspond to the start of the deceleration phase.

(ix) Ruffini et al. (2008) explain the early prompt and the steep-flat-steep phases within a unique scenario, a baryonic shell (fireshell) interacting with a non-homogeneous circumburst medium. The emission process is thermal at all times. Once the fireshell reaches a region of low density, ~ 0.03 – 2 pc away, it would decelerate very slowly, giving origin to the plateau phase.

It should be noted that the shallow phase is not ubiquitous: there are X-ray afterglows light curves where it is not detected. Therefore, any viable model should also explain the variety of the X-ray flux time behaviour. More importantly, all the above models propose that the X-ray shallow phase is due to afterglow emission (with the exception of the upscattering model by Panaitescu 2008). Thus, the same forward (or reverse) shock should produce optical radiation, which presumably would track the X-ray flux trend, including the shallow decay phase. This is not observed for some bursts which, therefore, challenge the above interpretation.

Ghisellini et al. (2007) instead suggested that the plateau phase of the X-ray (and sometimes optical) emission corresponds to a ‘late prompt’, namely due to the prolonged activity of the central engine (see also Lazzati & Perna 2007): after an early ‘standard’ prompt, the engine keeps producing shells of progressively lower power and bulk Lorentz factor for a long time (i.e. days). The dissipation during this and the early phases occurs at similar distances (close to the transparency radius). The reason for the shallow decay phase, and for the break ending it, is that the Γ -factors of the late shells are monotonically decreasing, allowing to see an increasing portion of the emitting surface, until all of it is visible. The break at T_A occurs when $\Gamma(t) = 1/\theta_j$. In our scenario, two independent emission components compete: the prevailing of the ‘late prompt’ versus a standard afterglow emission at different times can account for the variety of behaviours of X-ray and optical fluxes.

In this work, we thus try to model simultaneously both the X-ray and optical light curves as the sum of two components. The first one is the emission produced by the forward shock, according to the standard afterglow modelling. The second one is simply

parametrized, spectrally and temporally. Though we refer to it as ‘late prompt’ emission (which reflects our proposal), such a component could correspond to other interpretations. One of the aim of our investigation is to find the constraints that a more physical model must satisfy to give origin to this ‘late prompt’ component.

Throughout this paper, a Λ cold dark matter cosmology with $\Omega_M = 0.3$ and $\Omega_\Lambda = h = 0.7$ is adopted.

2 THE SAMPLE

All *Swift* bursts with known redshift, optical and X-ray follow up, as of end of 2008 March, were considered. Among them, we selected GRBs for which an estimate of the optical extinction at the host site appeared in literature.¹ This criterion is dictated by the need to determine reliable optical and X-ray intrinsic luminosities, in order to model their time-dependent behaviour. The corresponding sample comprises 33 bursts.

Information concerning these 33 GRBs are listed in Table 1, where we report: redshift, A_V^{host} , optical spectral indices β_o (corrected for extinction), X-ray spectral indices β_x (again accounting for absorption) and hydrogen column density N_H^{host} (at the host) as determined by fitting the X-ray spectrum.

It should be noted that usually A_V^{host} is determined by requiring that the intrinsic optical spectrum is a power law, and correcting the observed spectral curvature according to an extinction curve (the Small Magellanic Cloud one in most cases). Sometimes, however, the requirement adopted was that the optical and X-ray data lie on the same functional curve (being it a single or a broken power law). When multiple choices were available, estimates based on the optical data alone were preferred as the X-ray flux could belong to a different spectral component. For details on the host frame dust absorption determination for each GRB see the references in Table 1.

In order to compare the behaviour of different bursts, we dereddened the observed optical fluxes taking into account both the GRB host dust and the Galactic (Schlegel, Finkbeiner & Davis 1998) absorption along the line of sight. The reddening corrected fluxes have been then K -corrected and converted into monochromatic luminosities through

$$L(\nu_0) = \frac{4\pi d_L^2}{(1+z)^{1-\beta_o}} F(\nu_0), \quad (1)$$

where ν_0 is the central frequency of the photometric filter, d_L is the luminosity distance and β_o is the unabsorbed optical spectral index (see Table 1).

The X-ray light curves were taken from the UK Swift Science Data Centre² (see Evans et al. 2007 describing how the data were reduced). Also the X-ray 0.3–10 keV XRT (X-Ray Telescope) light curves have been corrected for the combined effects of both host frame N_H and Galactic column densities, using the unabsorbed spectral index β_x obtained from the X-ray spectral analysis (see Table 1). The unabsorbed 0.3–10 keV observer frame fluxes F_x have been converted to host frame 0.3–10 keV luminosities L_x as

$$L_x = \frac{4\pi d_L^2}{(1+z)^{1-\beta_x}} F_x. \quad (2)$$

For simplicity, we use the same β_x for the entire X-ray light curve, neglecting the sudden changes of β_x sometimes seen during X-ray flares, since the interpretation of the individual flares is beyond the

aim of this work. The analysis has been carried on in the GRB host time frame. We therefore rescale all the observed time intervals by $(1+z)^{-1}$.

3 THE MODEL

As mentioned we assume that at all times the flux is the sum of two components: the first one due to synchrotron radiation produced by the standard forward shock caused by the fireball running into the circumburst material and the second one is treated phenomenologically, since its form/origin is not currently known, though it can be possibly ascribed to the extension in time of the early prompt emission.

3.1 Forward shock component

Following the analytical prescriptions of Panaitescu & Kumar (2000), the forward shock emission depends on the following parameters.

- (i) E_0 – the (isotropic equivalent) kinetic energy of the fireball after it has produced the early prompt radiation.
- (ii) Γ_0 – the initial fireball bulk Lorentz factor. It controls the onset of the afterglow, but it does not influence the rest of the light curve. It is then rather undetermined when very early data are not available.
- (iii) n_0 or $\dot{M}_w/v_w - n_0$ is the value of the circumburst medium density if homogeneous, while \dot{M}_w/v_w (wind mass-loss rate over the wind velocity) determines the normalization of the density in the wind case ($\propto R^{-2}$) profile.
- (iv) ϵ_e – the ‘equipartition’ parameter setting the fraction of the available energy responsible for electron acceleration.
- (v) ϵ_B – the ‘equipartition’ parameter parametrizing the fraction of the available energy which amplifies the magnetic field.
- (vi) p – the slope of the relativistic electron energy distribution, as injected at the shock.

For simplicity, we assume that higher frequency of the afterglow synchrotron emission is beyond the X-ray range. These are six free parameters, if we consider n_0 or \dot{M}_w/v_w as a single one: in reality, the assumed homogeneous versus wind-like density profile can be considered as an additional degree of freedom.

3.2 Late prompt component

In the absence of a clear understanding of its origin, this component is parametrized with the only criterion of minimizing the number of free parameters. This can be considered as a first step towards a more physical modelling of this second component. A subsequent analysis of the parameters distribution could help us in constraining possible theoretical ideas. A first attempt in this direction will be discussed in Section 5.

The spectral shape – assumed to be constant in time – is described by a broken power law:

$$\begin{aligned} L_L(\nu, t) &= L_0(t) \nu^{-\beta_x}; & \nu > \nu_b \\ L_L(\nu, t) &= L_0(t) \nu_b^{\beta_o - \beta_x} \nu^{-\beta_o}; & \nu \leq \nu_b, \end{aligned} \quad (3)$$

where L_0 is a normalization constant. L_0 is not treated as a free parameter by taking it as the 0.3–10 keV luminosity L_{LX} of the late

¹ For one of them, GRB 070802, the photometric data set is not yet available.

² http://www.swift.ac.uk/xrt_curves/

Table 1. The sample. For all bursts, we report information taken from the literature (see the references), namely: redshift, optical extinction and hydrogen column density at the host (A_V^{host} and N_H^{host} , respectively), and the optical and X-ray indices found after de-absorbing. E_{iso} is in the 15–150 keV band, not K-corrected. T_{90} is in seconds, from the Swift catalogue (http://swift.gsfc.nasa.gov/docs/swift/archive/grb_table.html/).

GRB	z	A_V^{host}	β_o	β_X	N_H^{host}	$\log E_{\text{iso}}$	T_{90}	References
050318	1.44	0.68 ± 0.36	1.1 ± 0.1	1.09 ± 0.25	0.4 ± 0.1	52.11	32	Ber05a, Sti05, Per05
050319	3.24	0.11	0.59	0.73 ± 0.05	3.8 ± 2.2	52.31	152.5	Fyn05a, Kan08, Cus06
050401	2.8992	0.62 ± 0.06	0.5 ± 0.2	0.89 ± 0.03	16.0 ± 3	53.47	33.3	Fyn05b, Wat06, Wat06
050408	1.2357	0.73 ± 0.18	0.28 ± 0.33	1.1 ± 0.1	12.0 ± 3.5	52.18	15	Ber05b, DUP07, Cap07
050416A	0.653	0.19 ± 0.11	1.14 ± 0.2	1.04 ± 0.05	6.8 ± 1.0	50.69	2.5	Cen05, Hol07, Man07a
050525A	0.606	0.32 ± 0.2	0.57 ± 0.29	1.1 ± 0.25	1.5 ± 0.7	52.94	8.8	Fol05, Kan08, Blu06
050730	3.967	0	0.56 ± 0.06	0.87 ± 0.02	6.8 ± 1	53.19	156.5	Che05, Pan06, Per07
050801	1.56	0	0.6	0.87 ± 0.23	0 ± 0.5	51.25	19.4	DeP07, Kan08, DeP07
050802	1.71	0.55 ± 0.1	0.72 ± 0.04	0.88 ± 0.04	2.8 ± 0.5	52.16	19.0	Fyn05d Sch07, Oat07
050820A	2.612	0	0.77 ± 0.08	0.94 ± 0.07	6 ± 4	53.17	26.0	Pro05, Cen06a, Pag05
050824	0.83	0.14 ± 0.13	0.45 ± 0.18	1.0 ± 0.1	1.8 ± 0.65	50.68	22.6	Fyn05f, Kan08, Sol07
050922C	2.198	0	0.51 ± 0.05	0.89 ± 0.16	0.65 ± 0.27	52.98	4.5	Jak05a, Kan08, Ken05
051111	1.55	0.39 ± 0.11	1.1 ± 0.06	1.15 ± 0.15	8 ± 3	52.43	46.1	Hil05, Sch07, Gui07
060124	2.296	0	0.73 ± 0.08	1.06 ± 0.06	13 ± 4.5	53.6	750	Cen06b, Mis07, Rom06
060206	4.045	0 ± 0.02	0.73 ± 0.05	1.0 ± 0.3	0.4 ± 0.3	52.48	7.6	Fyn06, Kan08, Mor06
060210	3.91	1.14 ± 0.2	1.14 ± 0.03	1.14 ± 0.03	100 ± 12	53.14	255.	Cuc06, Cur07b, Cur07b
060418	1.489	0.25 ± 0.22	0.29 ± 0.04	1.04 ± 0.13	1.0 ± 0.4	52.72	103.1	Pro06, Ell06, Fal06
060512	0.4428	0.44 ± 0.05	0.99 ± 0.02	0.99 ± 0.02	0	50.12	8.5	Blo06, Sch07, Sch07
060526	3.221	0.04 ± 0.04	0.495 ± 0.144	0.8 ± 0.2	0	52.43	298.2	Ber06, Thö08, Cam06
060614	0.125	0.05 ± 0.02	0.81 ± 0.08	0.84 ± 0.08	0.15 ± 0.12	50.96	108.7	Pri06, Man07b, Man07b
060729	0.54	1.05	1.1	1.11 ± 0.01	1.9 ± 0.4	51.37	115.3	Thö06, Gru07, Gru07
060904B	0.703	0.44 ± 0.05	0.90 ± 0.04	1.16 ± 0.04	4.09 ± 0.13	51.40	171.5	Fug06, Kan08, Gru06
060908	2.43	0.055 ± 0.033	0.69	0.95 ± 0.15	0.64 ± 0.34	52.66	19.3	Rol06, Kan08, Eva06
060927	5.47	0.33 ± 0.18	0.64 ± 0.2	0.87	<0.34	52.82	22.5	Fyn06c, RuV07, RuV07
061007	1.26	0.48 ± 0.19	1.02 ± 0.05	1.01 ± 0.03	5.8 ± 0.4	53.33	75.3	Osi06, Mun07, Mun07
061121	1.314	0.72 ± 0.06	0.62 ± 0.03	0.87 ± 0.08	9.2 ± 1.2	52.85	81.3	Blo06, Pag07, Pag07
061126	1.1588	0	0.93 ± 0.02	1.00 ± 0.07	11 ± 0.7	53.08	70.8	Per08a, Per08a, Per08a
070110	2.352	0.08	1.1 ± 0.1	1.1 ± 0.1	2.6 ± 1.1	52.37	88.4	Jau07, Tro07, Tro07
070125	1.547	0.11 ± 0.4	0.58 ± 0.1	1.1 ± 0.1	2 ± 1	54.08	65	Fox07, Kan08, Upd08
071003	1.1	0.209 ± 0.08	0.93 ± 0.04	1.14 ± 0.12	1.1 ± 0.4	52.28	150	Per07, Per08b, Per08b
071010A	0.98	0.615 ± 0.15	0.76 ± 0.25	1.46 ± 0.2	17.4 ± 4.5	50.7	6	Pro07, Cov08a, Cov08a
080310	2.42	0.1 ± 0.05	0.6	0.9 ± 0.2	7.0 ± 1	52.49	365	Pro08, PeB08, Bea08
080319B	0.937	0.07 ± 0.06	0.33 ± 0.04	0.814 ± 0.013	1.87 ± 0.13	53.27	50	Vre08, Blo08, Blo08

References: Ber05a: Berger & Mulchaey (2005); Sti05: Still et al. (2005); Per05: Perri et al. (2005); Fyn05a: Fynbo et al. (2005a); Kan08: Kann et al. (2008); Cus06: Cusumano et al. (2006); Fyn06: Fynbo et al. (2005b); Wat06: Watson et al. (2006); Ber05b: Berger, Gladders & Oemler (2005); DUP07: de Ugarte Postigo (2007); Cap07: Capalbi et al. (2007); Cen05: Cenko et al. (2005); Hol07: Holland et al. (2007); Man07a: Mangano et al. (2007a); Fol05: Foley et al. (2005); Blu06: Blustin et al. (2006); Che05: Chen et al. (2005); Pan06: Pandey et al. (2006); Per06: Perri et al. (2006); DeP07: De Pasquale et al. (2007); Fyn05d: Fynbo et al. (2005d); Sch07: Schady et al. (2007); Oat07: Oates et al. (2007); Pro05: Prochaska et al. (2005); Cen06a: Cenko et al. (2006a); Pag05: Page et al. (2005); Fyn05f: Fynbo et al. (2005f); Sol07: Sollerman et al. (2007); Jak05a: Jakobsson et al. (2005a); Ken05: Kennea et al. (2005); Hil05: Hill et al. (2005); Gui07: Guidorzi, Gomboc & Kobayashi (2007); Cen06b: Cenko, Berger & Cohen (2006b); Rom06: Romano et al. (2006); Fyn06: Fynbo et al. (2006a); Mor06: Morris et al. (2006); Cuc06: Cucchiara, Fox & Berger (2006); Cur07b: Curran et al. (2007b); Pro06: Prochaska et al. (2006); Ell06: Ellison et al. (2006); Fal06: Falcone et al. (2006); Blo06: Bloom et al. (2006a); Ber06: Berger & Gladders (2006); Tho06: Thöene et al. (2006); Cam06: Campana et al. (2006a); Pri06: Price, Berger & Fox (2006); Man07b: Mangano et al. (2007b); Thö06: Thöene et al. (2006); Gru07: Grupe et al. (2007); Fug06: Fugazza, D’Avanzo & Malesani (2006); Gru06: Grupe et al. (2006); Rol06: Rol et al. (2006); Eva06: Evans et al. (2006); Fyn06c: Fynbo et al. (2006c); RuV07: Ruiz-Velasco et al. (2007); Osi06: Osip, Chen & Prochaska (2006); Mun07: Mundell et al. (2007); Blo06: Bloom, Perley & Chen (2006b); Pag07: Page et al. (2007); Per08a: Perley et al. (2008a); Jau07: Jaunsen et al. (2007); Tro07: Troja et al. (2007), Fox et al. (2007); Upd08: Updike et al. (2008); Per07: Perley et al. (2007); Per08b: Perley et al. (2008b); Pro07: Prochaska et al. (2007); Cov08: Covino et al. (2008a); Pro08: Beardmore et al. (2008), PeB08: Perley & Bloom (2008a), Prochaska et al. (2008); Vre08: Vreeswijk et al. (2008) and Blo08: Bloom et al. (2008).

prompt emission at the time T_A :

$$L_{\text{LX}}(T_A) = \int_{0.3}^{10} L_{\text{L}}(\nu, T_A) d\nu \quad (4)$$

with ν in keV. Again for simplicity, we assume that any cut-off frequency, at high as well as at low energies, is outside the infrared-optical (IR-optical)/X-ray frequency range.

The temporal parameters, described by the flat and steep decay indices, α_{fl} and α_{st} , respectively, and the time T_A at which the two behaviours join, are assumed to be described by a smooth broken

power law:

$$L_{\text{L}}(\nu, t) = L_{\text{L}}(\nu, T_A) \frac{(t/T_A)^{-\alpha_{\text{fl}}}}{1 + (t/T_A)^{\alpha_{\text{st}} - \alpha_{\text{fl}}}}. \quad (5)$$

To summarize the free parameters reproducing the late prompt emission are as follows.

- (i) β_X – the spectral index of the late prompt emission in X-rays.
- (ii) β_o – the spectral index of the late prompt emission in the IR-optical.

- (iii) ν_b – the break frequency between the optical and the X-rays.
- (iv) $L_{LX}(T_A)$ – the 0.3–10 keV luminosity of the late prompt emission at the time T_A .
- (v) α_n – the decay index for the shallow phase, before T_A .
- (vi) α_{st} – the decay index for the steep phase, after T_A .
- (vii) T_A – the time when the shallow phase ends.

These are seven free parameters. It is worth stressing that, despite of their number, these are rather well constrained by observations. When the late prompt emission dominates, α_n , α_{st} , T_A can be directly determined as well as one spectral index (usually β_X , since the late prompt emission is usually dominating in the X-ray range). Some degeneracy is present between ν_b and β_o , both of which control the importance of the optical flux due to the late prompt component: the same optical flux can, for instance, be reproduced assuming a steeper (flatter) β_o and a larger (smaller) ν_b , as the ratio between the 0.3 and 10 keV X-ray luminosity and the $\nu_o L(\nu_o)$ optical luminosity of the late prompt is proportional to $\nu_b^{\beta_X - \beta_o}$.

3.3 Caveats

As our treatment is necessarily simplified, simply parametrizing the late prompt emission, we analyse below the most important (or drastic) assumptions, trying to outline their effects.

(i) The afterglow calculations are based on the prescriptions by Panaitescu & Kumar (2000). In their analytical treatment, the curvature of the emitting shell is neglected. The inclusion of the time delay between the emission times of photons received at any observer time would smooth out any relatively sharp feature of the light curve (especially when the injection or cooling frequency crosses the considered band). However, the derived light curves are sufficiently accurate for the purposes of this work.

(ii) Almost all of the calculations of the afterglow light curves assume that ϵ_e and ϵ_B are constant in time. This is likely to be just a rough approximation, since the physical conditions at the shock front change in time (Γ as well as the density measured in the comoving frame do change). As such a temporal dependence is not known or predicted, we are forced to adopt this simplification.

(iii) The afterglow emission is assumed to be isotropic, *therefore no jet breaks* can be reproduced in the calculated light curves.

(iv) The spectrum of the late prompt emission is assumed to be constant in time, in the observer frame. This is likely to be the most critical approximation, adopted just to minimize the number of free parameters. One might speculate that if this component originate by shells with decreasing bulk Lorentz factor (as in the models by Genet et al. 2007; Ghisellini et al. 2007; Uhm & Beloborodov 2007), then it is likely that the observed break frequency ν_b would also decrease in time (if constant in the comoving frame). While this would not affect the X-ray light curves (if ν_b is below the X-ray window even at early times), the optical emission would become relatively more important as time goes on. For instance, a plateau in the X-rays could correspond to a rising optical light curve. This suggests a possible observational test. Assume to select a burst in which both the optical and the X-ray light curves are dominated by the late prompt emission. If ν_b decreases in time, we should see two effects. First, the optical plateau should be shallower than the X-ray one (since the X-ray to optical flux ratio decreases as $\nu_b^{\beta_X - \beta_o}$). Secondly, when ν_b crosses the optical band, we should see a spectral

steepening, since the decreasing ν_b acts as a cooling break. After ν_b has crossed the optical band, the optical and the X-ray fluxes should lie on the same power law.

(v) The low- and high-frequency cut-offs of both the afterglow and late prompt emission have been neglected as free parameters. The late emission spectrum might have a high-frequency cut-off in the X-ray band. Given the current status of the X-ray observations, that do not detect such a cut-off, this simplification is reasonable.

(vi) The late prompt emission is assumed to last forever, while, of course, it will die away after some time. This may happen, however, at very late times, when any X-ray or optical observations are not any longer feasible or when the GRB emission cannot be detectable (in the optical, emission can be dominated by the host galaxy or sometimes by a supernova associated to the burst).

(vii) Flares, re-brightenings and/or bumps in the light curve are not accounted for. In our scenario, these are separated components, though in practice, their presence makes the choice of what data points to ‘fit’ a bit subjective.

A final remark. Due to the above caveats, the values of the parameters for a single source may be subject to rather large uncertainties. In this sense, the *distributions* of parameter values are much more meaningful. We could badly model an individual source, but the general conclusions could be right, if some coherence is found for the parameters of the entire sample.

4 RESULTS

Figs 1–9 show the X-ray and optical light curves of the 33 GRBs together with the results of the modelling: dotted lines refer to the late prompt emission, dashed ones to the afterglow component and the solid lines to their sum.

The parameters inferred from the modelling of the light curves are reported in Table 2, together with a tentative classification of the bursts according to the dominant contribution: ‘A’ stands for afterglow, ‘L’ for late prompt and ‘X’ and ‘O’ refer for X-ray and optical, respectively. For instance, XL–OA indicates that the X-ray flux is dominated by the late prompt, and the optical by the afterglow. When both type of emissions are comparable, we use ‘M’, for mix. This also comprises the case when one component dominates in one time interval, and the other in another time interval. The number of bursts which can be described within these categories is summarized in Table 3. The X-ray flux is dominated by the late prompt emission or a mixture of late prompt and afterglow for the majority of GRBs, the opposite being true for the optical emission. Out of our 33 events, the most common cases are XM–OA (10 GRBs, namely a mix in the X-rays and afterglow in the optical) and XL–OM (eight GRBs, namely late prompt in the X-rays and a mix in the optical).

The overall result is that both components have comparable relevance in most cases. This can be seen as a direct consequence of the different slopes of the light curves: since the late prompt emission is flatter than the afterglow up to T_A , and often steeper after this time, it is likely that the late prompt emission dominates or contributes around T_A even in the optical. Conversely, the afterglow may dominate or be important at very early and late times (if there is no jet break). In other words, the similar contribution of both the components is the cause of the complex X-ray–optical behaviour observed.

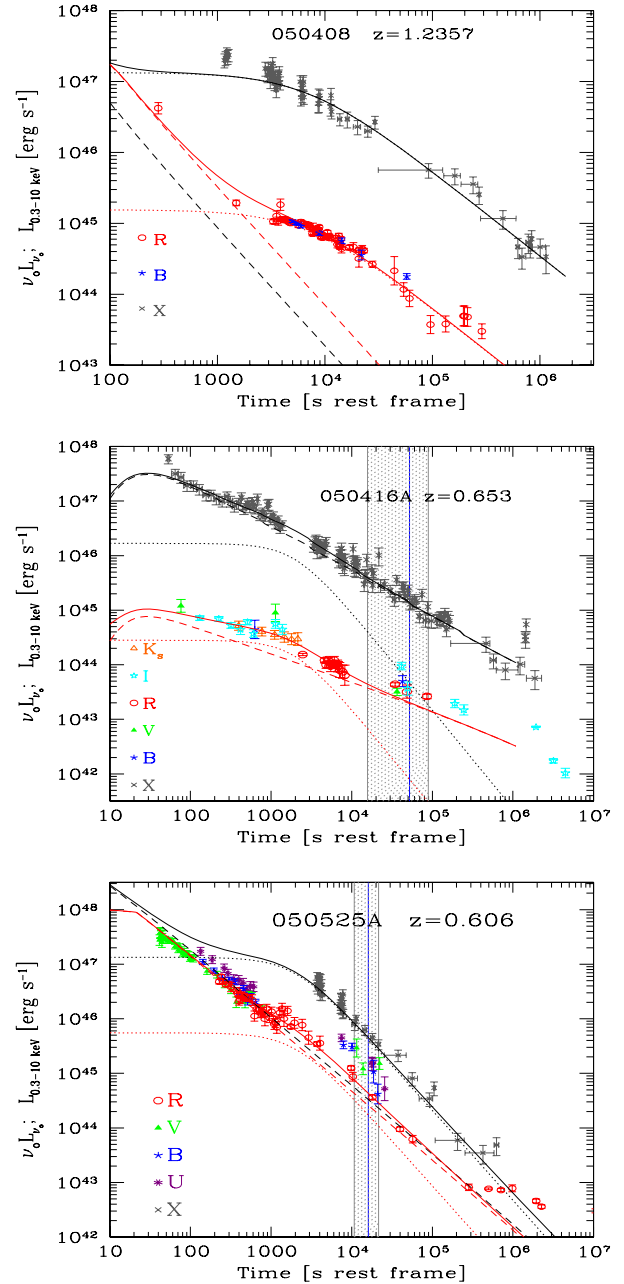
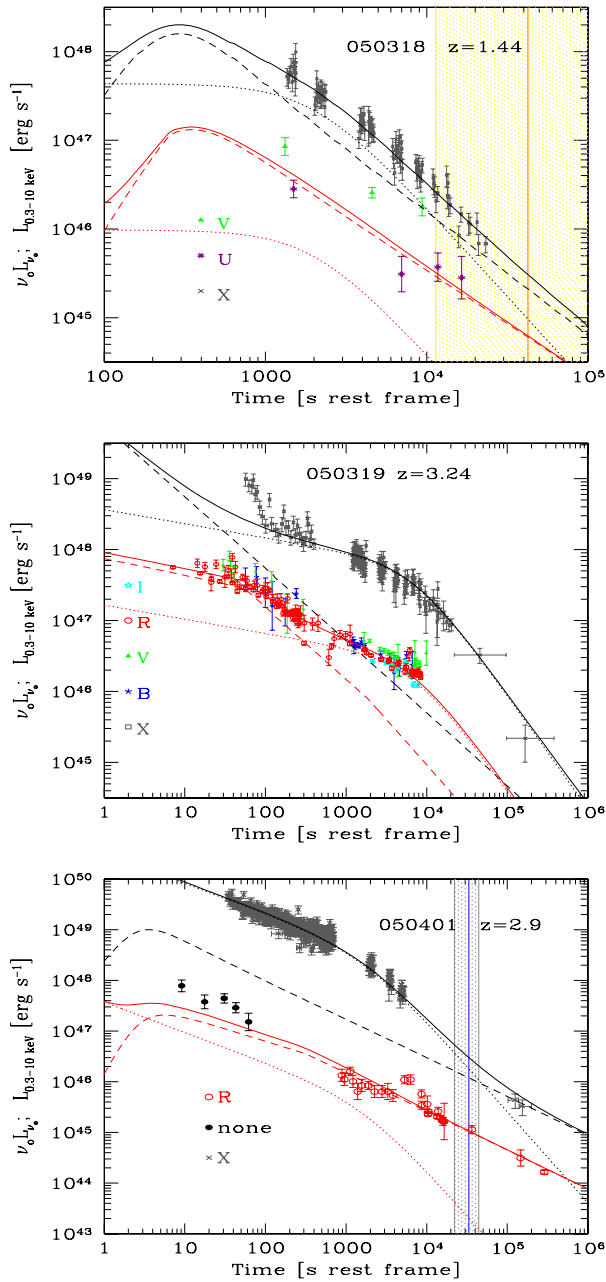


Figure 1. Figs 1–9. X-ray (in grey) and optical (different symbols, as labelled) light curves. Lines indicate the model fitting: afterglow (dashed line), late prompt (dotted line) and their sum (solid line). Black lines refer to the X-rays, light grey (red in the electronic version) for the optical. The vertical line (and shaded band) corresponds to the rest-frame jet break times (and their 3σ uncertainty). Grey lines and stripes correspond to jet break times as reported in the literature (references are listed in Ghirlanda et al. 2007), light grey (yellow in the electronic version) lines and stripes refer to jet times expected if the burst followed the Ghirlanda relation. These are shown only for bursts with measured E_{peak} , the peak energy of the prompt emission. References for the optical data can be found in the appendix.

4.1 Distribution of parameters

Figs 10 and 11 show the distribution of all our input parameters. For comparison, in these figures we report the values found by

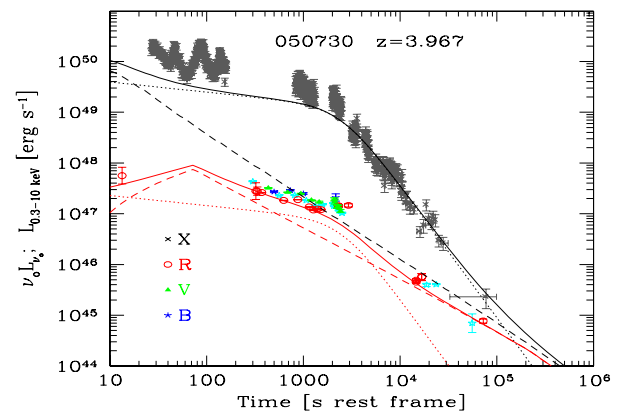


Figure 2. Same as in Fig. 1.

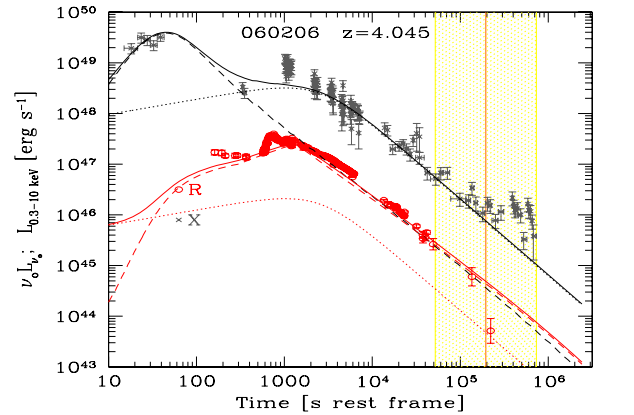
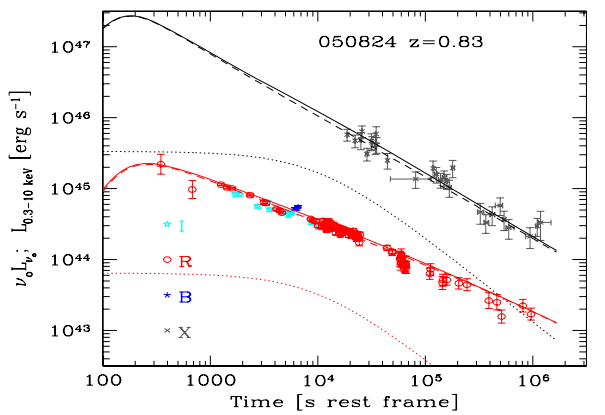
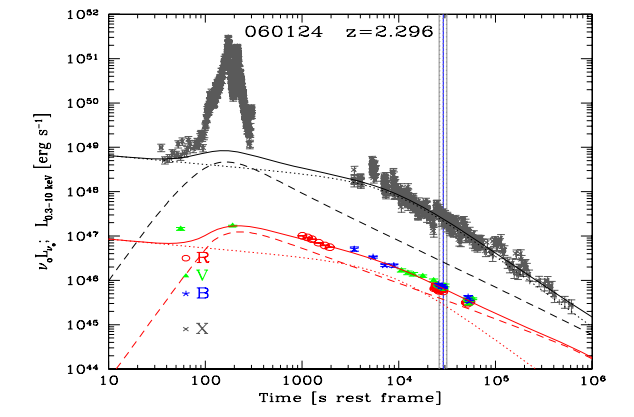
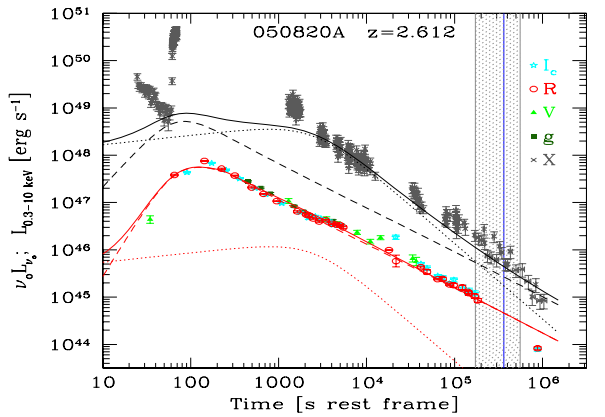
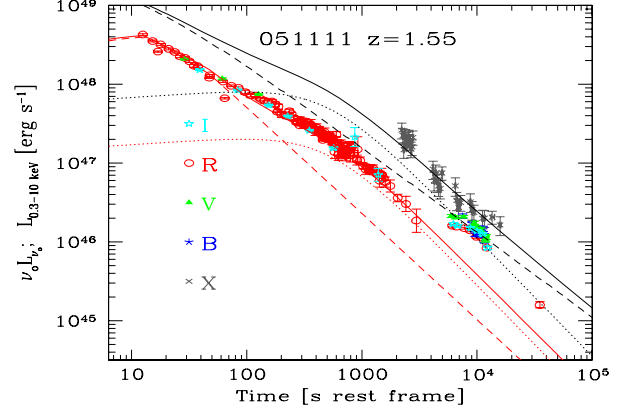
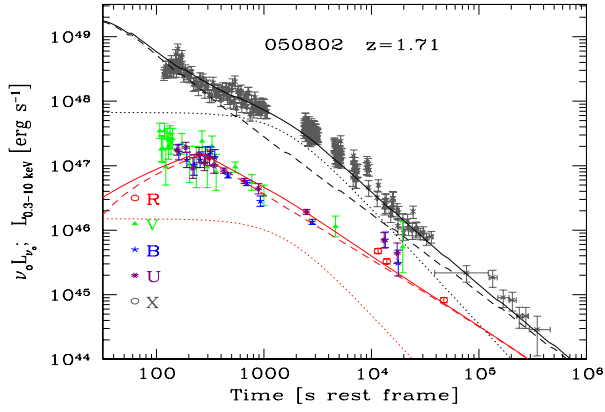
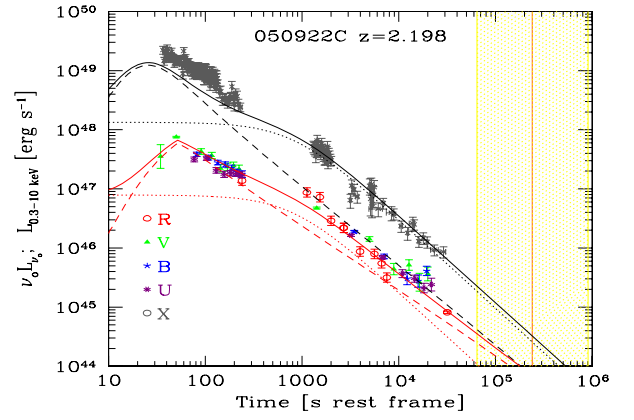
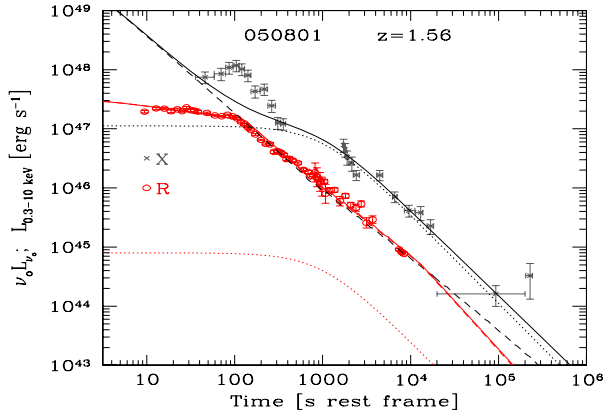


Figure 3. Same as in Fig. 1.

Figure 4. Same as in Fig. 1.

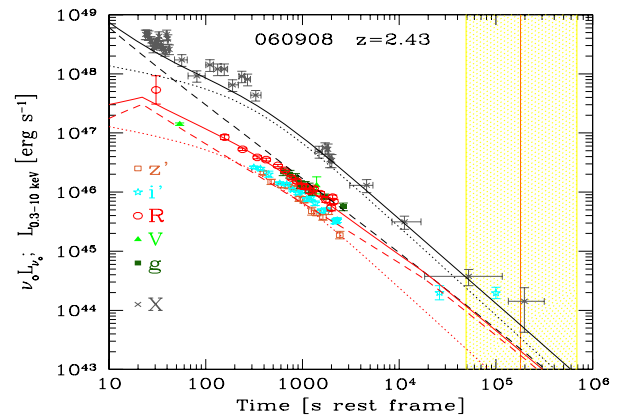
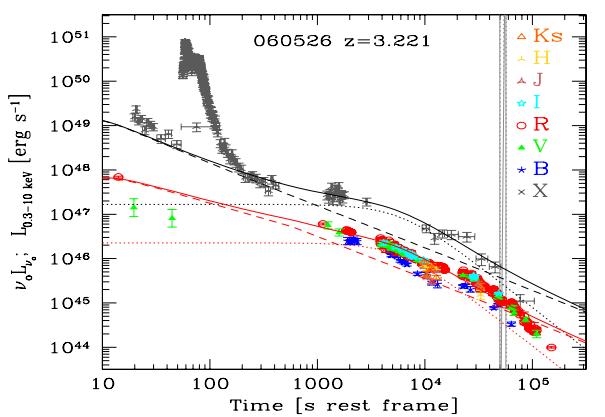
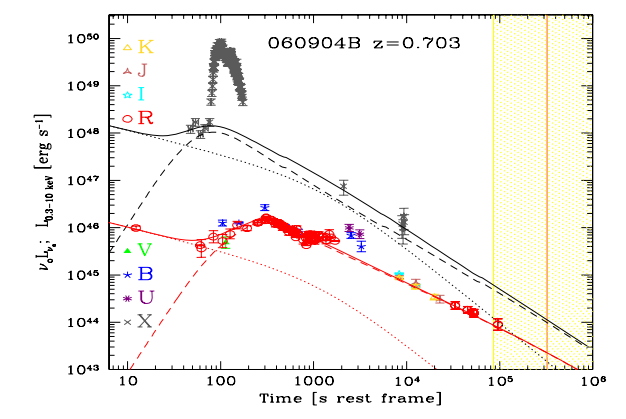
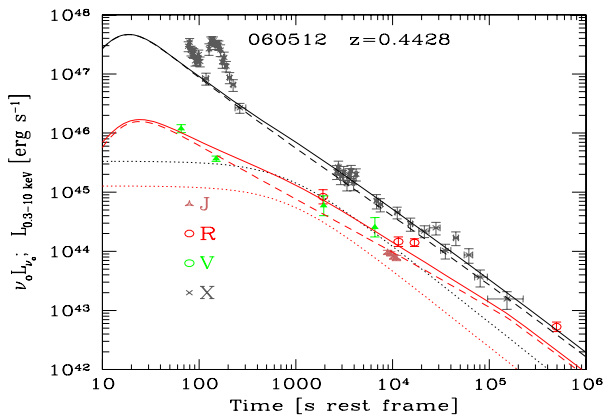
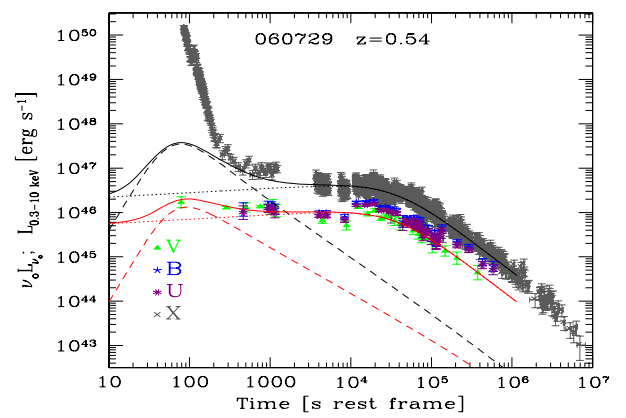
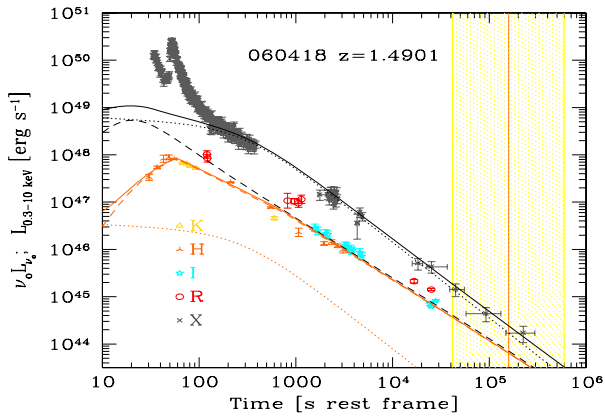
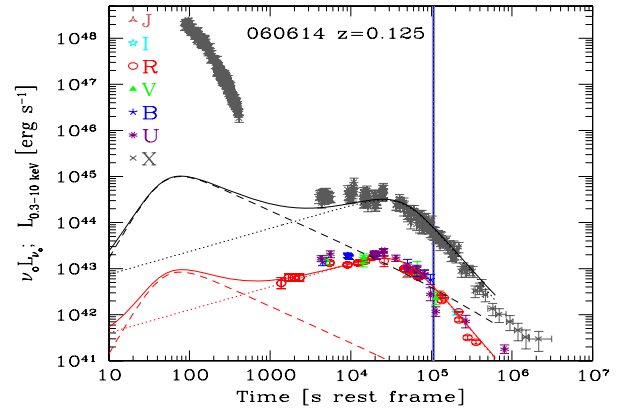
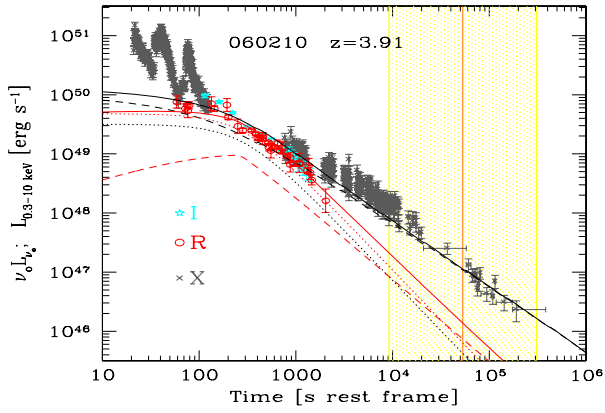


Figure 5. Same as in Fig. 1.

Figure 6. Same as in Fig. 1.

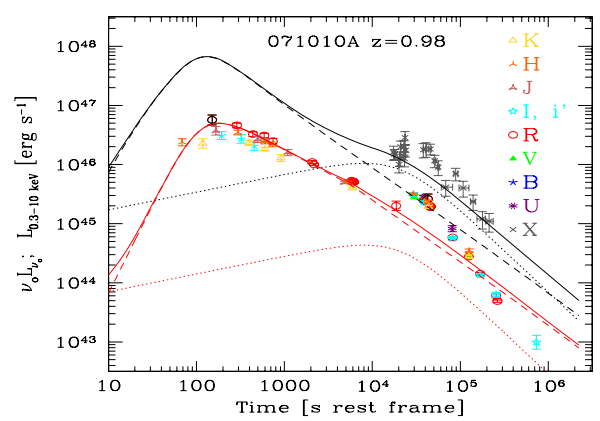
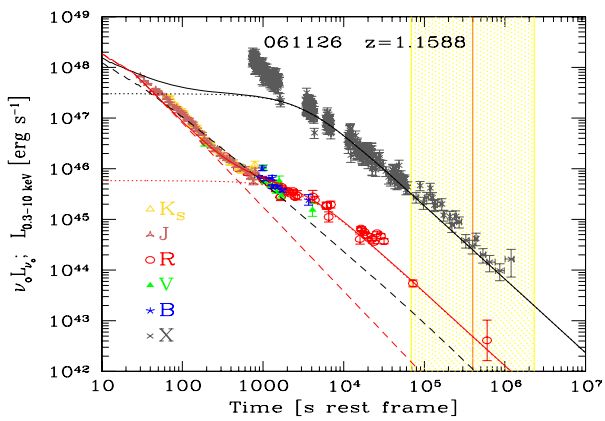
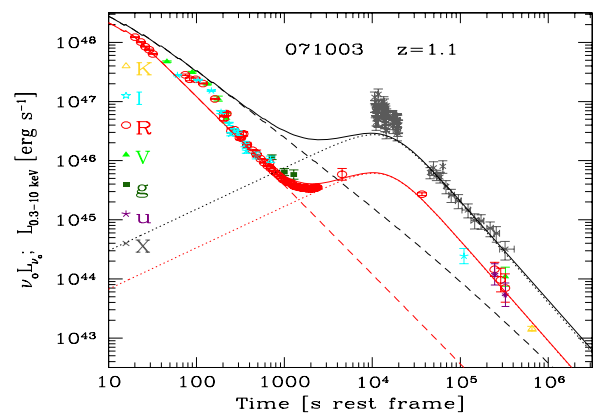
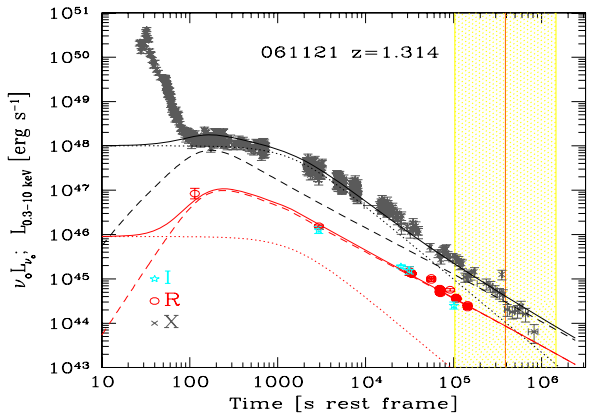
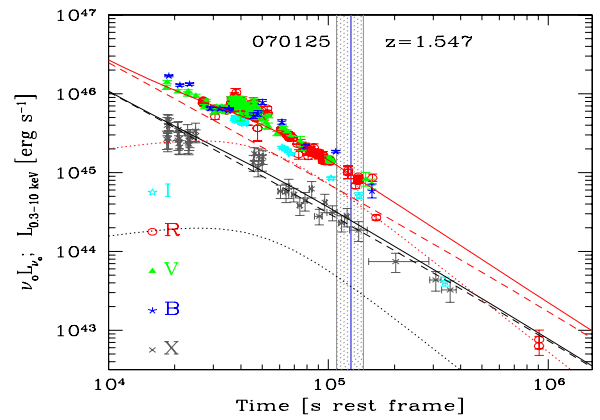
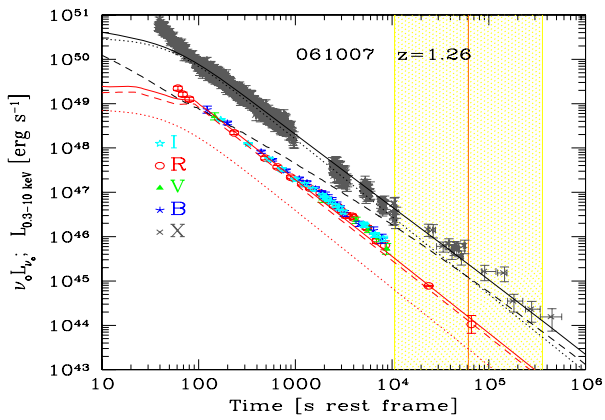
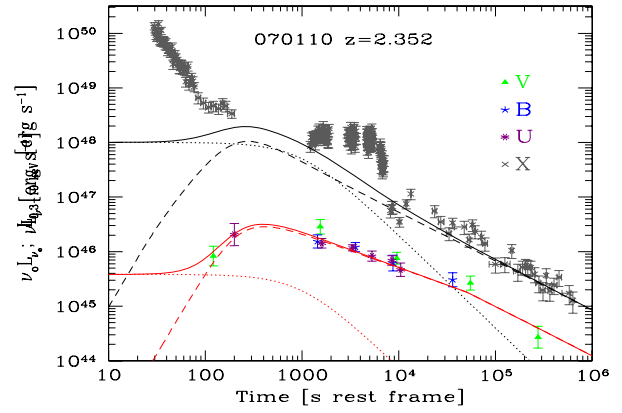
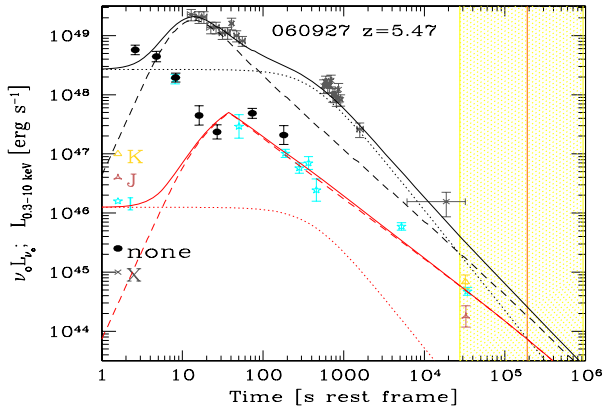


Figure 7. Same as in Fig. 1.

Figure 8. Same as in Fig. 1.

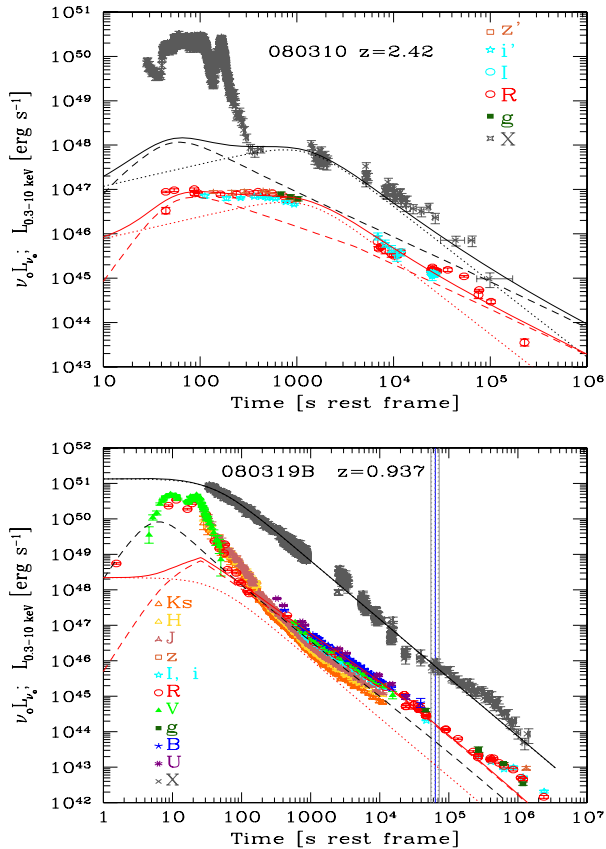


Figure 9. same as in Fig. 1.

Panaitescu & Kumar (2002) for 10 pre-Swift bursts.³ In our interpretation the X-ray luminosity in the majority of cases is not produced by the afterglow, which is thus less energetic.

Most (25 out of 33) afterglows can be consistently described by the interaction of the fireball with a homogeneous medium. This is especially the case when the optical light curve indicates the onset of the afterglow itself (i.e. a very early rising phase), that cannot be reproduced with a wind-like density profile. The latter, in fact, produces almost flat optical light curves in the early phases. The homogeneous densities are very narrowly distributed around a mean value of $\langle n_0 \rangle \sim 3 \text{ cm}^{-3}$. For eight GRBs (see Table 2), a better modelling can be achieved invoking a wind-like density profile. All but one of these eight bursts can be modelled with a value of the ratio of the mass-loss rate and the wind velocity of $\dot{M}_w/v_w = 10^{-8} (M_\odot \text{ yr}^{-1}) / (\text{km s}^{-1})$ that can correspond to $\dot{M}_w = 10^{-5} M_\odot \text{ yr}^{-1}$ and $v_w = 10^3 \text{ km s}^{-1}$. The remaining burst requires

³ Panaitescu & Kumar (2002) give the collimation corrected value for the isotropic kinetic energy of the fireball after the early prompt phase. We have then divided this value by $(1 - \cos \theta_j)$ to get the isotropically equivalent value of E_0 to be compared with the values found for our bursts. Note that Γ_0 does not affect the properties of the afterglow after its onset, and is therefore not an important parameter for Panaitescu & Kumar (2002), who are fitting data taken much later than the afterglow onset (with the exception of GRB 990123). The afterglow parameters found for our bursts are rather standard, being similar to the ones obtained by Panaitescu & Kumar (2002) (see also Panaitescu & Kumar 2001a,b). The distribution of the circumburst density n_0 is narrower for the bursts in our sample, while the distributions of ϵ_e and ϵ_B are centred on smaller values.

half of this value. Similarly to what had been found by Panaitescu & Kumar (2002), the afterglow parameters distribution is quite broad, i.e. they do not cluster around typical values. Exceptions are the density n_0 and the bulk Lorentz factor Γ_0 .

Also the distributions of some late prompt parameters (i.e. T_A , L_{T_A} and v_b) are rather broad, while β_0 and the temporal slopes α_{fl} and α_{st} are more narrowly distributed. The values of T_A range from 10^2 to 10^4 s or more (in the rest frame), and are (anti)correlated with the late prompt luminosity at T_A , as shown in Fig. 12. This confirms the correlation found by Dainotti, Cardone & Capozziello (2008). This results in a narrow distribution of $T_A L_{T_A}$ (Fig. 11).

The distributions of β_0 and v_b must be taken with caution, since the model fixes only their combination, and only in a few GRBs they can be constrained separately (i.e. when the optical light curve is dominated by the late prompt emission and the spectral index during this phase is known).

The distribution of α_{st} is intriguing, since it is centred around a mean value of 1.6. This is very close to $5/3$, the predicted decay of the accretion rate of fall-back material (see also Section 5 where this point is discussed in more depth). The values of α_{fl} cluster around 0.

In Fig. 11, we show the distribution of $T_A L_{T_A}$, and in Fig. 13 we show $T_A L_{T_A}$ as a function of E_{iso} . The two quantities are correlated (albeit poorly) and the energy contained in the late prompt emission (of which $T_A L_{T_A}$ is a proxy) is at most comparable with E_{iso} . More frequently $T_A L_{T_A}$ is one or two orders of magnitude smaller than E_{iso} , in agreement with the findings by Willingale et al. (2007).

Fig. 11 also shows the distribution of $E_{iso}/(E_0 + E_{iso})$. This ratio represents η , the fraction of the total energy of the fireball required to produce the observed early prompt radiation. In Fig. 14, this fraction is shown as a function of E_{iso} . Although there is a weak positive correlation, the mean value is well defined and corresponds to $\eta \sim 0.1$.

4.2 Jet breaks

A currently hot debate concerns the absence of jet breaks in the light curves of GRB afterglows. In the scenario we propose, the light curve comprises two components of which only the afterglow one should present a jet break (at t_j). It follows that jet breaks should be more often detectable in the optical, rather than being achromatic, and the after-break slopes may be shallower than predicted by the closure relations.

(i) No jet breaks. When the flux is dominated by the late prompt emission in both the optical and X-ray bands, jet breaks may become unobservable. The late prompt emission (at least after a few thousand seconds) does so for six GRBs of the sample (namely GRB 050319, GRB 050408, GRB 060614, GRB 060729, GRB 061126 and GRB 071003). Therefore, for these bursts, no jet break is predicted to be visible if the late prompt light curve continues unbroken for a long time – if the late prompt component instead breaks, we might erroneously interpret this as a jet break.

(ii) Achromatic jet breaks. Viceversa, an achromatic jet break should be observed when both in the optical and X-ray light curves the afterglow emission prevails, at least when the jet break is likely to occur. 16 GRBs of the sample could show such an achromatic break (GRB 050318, GRB 050401, GRB 050416A, GRB 050802, GRB 050820A, GRB 050824, GRB 060512, GRB 060904B, GRB 060908, GRB 060927, GRB 061121, GRB 070110, GRB 070125, GRB 071010A, GRB 080310 and GRB 080319B). Emission in several of these bursts – although dominated by afterglow emission,

Table 2. Input parameters for the afterglow component (columns 2–7) and the late prompt emission (columns 8–14). Column 1: burst Id; column 2: fireball kinetic energy (after the early prompt emission, in units of 10^{53} erg); column 3: initial bulk Lorentz factor; column 4: density of circumburst medium: values equal or larger than 1 are for a homogeneous density; values much smaller than 1 correspond to a wind-like profile; the listed value is \dot{M}_w/v_w , where \dot{M}_w is the mass-loss rate in $M_\odot \text{ yr}^{-1}$ and v_w is the wind velocity in km s^{-1} . Columns 5 and 6: equipartition parameters ϵ_e and ϵ_B ; Column 7: slope of the assumed relativistic electron distribution; column 8: spectral break of the late prompt emission (in Hz); columns 9 and 10: high- and low-energy spectral indices of the late prompt emission; columns 11 and 12: decay slopes of the late prompt emission, before and after T_A listed in column 13 (in sec); column 14: luminosity (in units of 10^{45} erg s^{-1}) in the 0.3–10 keV energy range of the late prompt emission, at the time T_A and column 15: burst classification (see the text).

GRB	$E_{0,53}$	Γ_0	n_0	ϵ_e	ϵ_B	p	ν_b	β_X	β_o	α_{fl}	α_{st}	T_A	L_A	Class
1	2	3	4	5	6	7	8	9	10	11	12	13	14	15
050318	10	100	2	1.e-2	2.2e-4	2.5	1.e16	1.1	0.0	0.0	2.0	2.e3	434	XM–OA
050319	0.5	300	1.e-8	1.e-2	1.e-4	2.	1.e15	0.75	0.6	0.2	1.6	7.e3	623	XL–OM; XA early
050401	1.2	350	10	1.e-4	1.e-2	1.65	7.e16	0.9	−0.1	0.6	1.8	1.75e3	3.7e3	XM–OA
050408	2	200	3	1.e-3	3.e-2	2.8	6.e16	1.1	0.28	0.0	1.2	7.e3	133	XL–OM
050416A	0.6	200	3	1.e-4	8.e-5	1.67	7.e16	1.1	0.4	0.0	1.8	2.e3	17	XA–OA
050525A	1	100	1.e-8	1.e-3	2.e-2	2.3	5.e15	1.1	0.0	0.0	1.65	2.e3	133	XL–OA; XA early
050730	5	300	8	5.e-3	7.e-4	2.3	4.e16	0.9	0.15	0.2	2.6	2.5e3	1.3e4	XL–OM; XA late
050801	0.2	100	1.e-8	1.5e-2	7.e-4	2.4	2.e16	0.9	0.1	0.0	1.5	1.e3	112	XL–OA; XA early
050802	3	200	3	2.e-2	2.e-4	2.3	1.e16	1.1	0.0	0.0	1.8	1.5e3	667	XM–OA
050820A	4	120	10	1.e-3	1.e-2	1.85	5.e16	1.1	0.0	−0.2	1.6	2.5e3	5.e3	XM–OA
050824	0.7	100	1	2.e-4	3.e-3	1.75	1.e16	1.1	0.0	0.0	1.2	1.e4	3.33	XA–OA
050922C	10	250	2	2.e-3	1.2e-3	2.4	2.e16	1.1	0.5	0.0	1.5	8.e2	1334	XL–OM; XA early
051111	5	120	5.e-9	1.e-3	1.e-3	2.1	2.e15	1.1	0.5	−0.1	1.5	5.e2	1.e3	XM–OM
060124	5	110	3	5.e-3	6.e-4	2.	2.e16	1.1	0.1	0.2	1.6	9.e3	1.7e3	XL–OM; XA early
060206	4	180	2	5.e-2	6.e-4	2.6	4.e16	1.1	0.1	−0.3	1.5	2.5e3	5.e3	XL–OM
060210	80	100	1.e-8	5.e-3	8.e-4	2.15	1.5e16	1.25	1.25	0.0	1.7	2.8e2	3.1e4	XA–OL
060418	5	200	10	1.e-3	1.e-2	2.3	2.e16	1.1	0.1	0.1	1.6	2.8e2	4.3e3	XL–OA
060512	3	200	10	1.2d-4	1.e-3	2.15	1.e15	1.1	0.5	0.0	1.3	8.e2	3.33	XA–OA
060526	4	300	10	3.e-4	6.e-3	1.9	8.e15	1.1	0.6	0.0	1.9	6.e3	167	XM–OM
060614	0.03	100	1	2.e-3	2.e-5	2.	5.e16	1.1	0.6	−0.5	2.1	4.5e4	0.5	XL–OL; XA–OA early
060729	0.5	110	3	4.e-3	1.e-3	2.3	2.e15	1.1	0.5	−0.1	1.4	3.5e4	50	XL–OL; XA–OA early
060904B	0.3	100	3	2.8e-2	4.e-4	2.15	2.e16	1.1	0.0	0.5	1.6	1.3e3	100	XM–OA; OL early
060908	1	400	10	2.e-3	3.e-3	2.3	6.e15	1.1	0.4	0.3	1.5	3.e2	500	XM–OA
060927	8	220	30	3.e-3	1.e-4	2.3	3.e16	1.1	0.0	0.0	1.7	4.e2	2.7e3	XM–OA
061007	60	200	1.e-8	3.e-3	3.e-4	2.6	8.e15	1.1	0.0	0.0	1.75	5.e1	3.e5	XM–OA
061121	6	110	3	4.e-4	1.e-2	2.	2.e16	1.1	0.0	0.0	1.65	1.5e3	1.e3	XM–OA
061126	3	100	1.e-8	1.e-3	2.e-4	2.5	1.e16	1.1	0.0	0.0	1.45	3.e3	300	XL–OM
070110	3	100	1	5.e-4	6.e-3	1.8	5.e16	1.1	0.0	0.0	1.7	1.e3	1.e3	XA–OA
070125	4	300	1	1.3e-2	6.e-2	2.65	1.e15	1.6	1.6	−0.4	2.2	5.e4	0.3	XA–OM
071003	4	100	1.e-8	1.e-3	1.5d-4	2.3	1.e16	1.1	0.8	−0.7	1.7	1.5e4	50	XL–OM; XA early
071010A	5	120	3	3.e-4	6.e-3	2.	5.e15	1.1	0.0	−0.3	1.4	2.e4	17	XL–OA; XA early
080310	1	120	6	1.e-3	7.e-3	1.95	1.e16	1.1	0.4	−0.5	1.7	1.3e3	1.3e3	XM–OA; OM mid
080319B	50	400	10	1.e-3	8.e-4	2.7	6.e16	1.1	−0.1	0.0	1.65	4.e1	1.3e6	XL–OA

Table 3. Number of sources dominated by different components: XA (OA): X-ray and optical flux dominated by the afterglow emission; XL (OL): X-ray and optical flux dominated by the late prompt emission and XM (OM): X-ray and optical fluxes where the late prompt and afterglow emission are relevant.

XL	15	
XA	6	
XM	12	
OL	3	
OA	19	
OM	11	
XL–OL	2	Both with XA–OA very early
XA–OA	4	
XM–OM	2	
XL–OA	5	Three bursts with XA early
XA–OL	1	
XM–OL	0	
XM–OA	10	One with OL early, one with OM mid
XA–OM	1	
XL–OM	8	Four with XA early, 1 with XA very late

especially in the X-ray band, at late times – still comprises a relevant contribution from the late prompt component. Therefore, the steepening of their light curve after t_j should be shallower than what the standard afterglow theory predicts.

(iii) Chromatic jet breaks. When the late prompt is dominating in one band, and the afterglow in the other, a jet break should be visible only in the afterglow-dominated band. According to our findings, a jet break could be present in the optical but not in the X-rays band in nine GRBs (GRB 050525A, GRB 050730, GRB 050801, GRB 050922C, GRB 060124, GRB 060206, GRB 060418, GRB 060526 and GRB 061007). Instead, two GRBs (GRB 051111 and GRB 060210) could show a jet break in X-rays but not in the optical.

In Figs 1–9, we indicate the time at which a jet break has been reported to be detected or the time at which a jet break is expected to be seen if the burst were to follow the $E_{\text{peak}}-E_\gamma$ (Ghirlanda) relation (Ghirlanda, Ghisellini & Lazzati 2004, updated in Ghirlanda et al. 2007) (see the figure caption). The latter ones are estimated only for

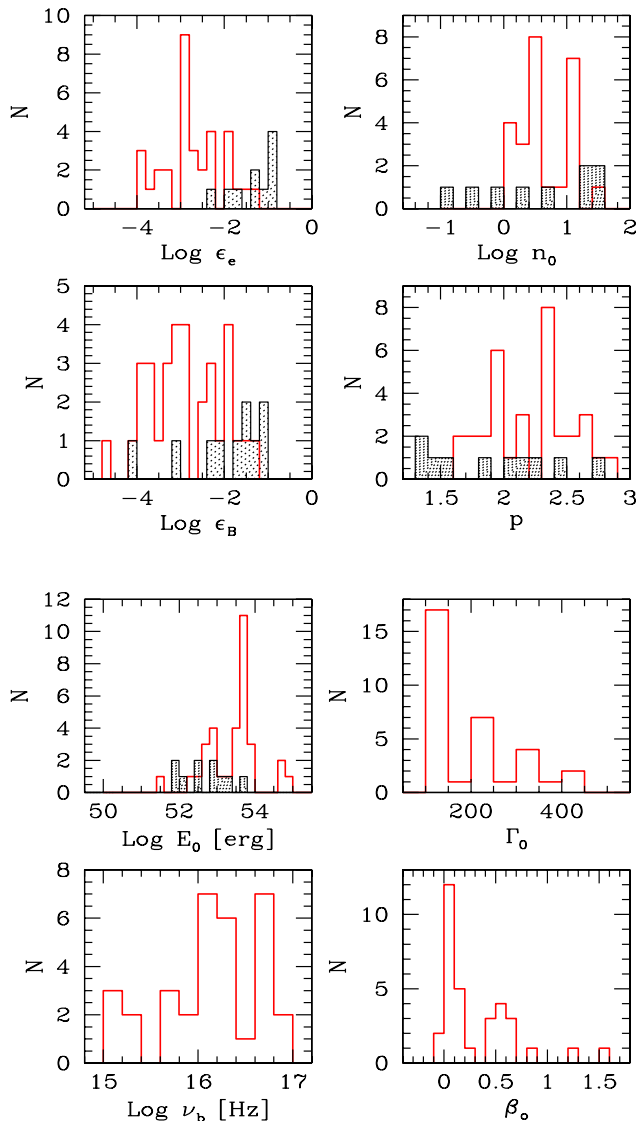


Figure 10. Top four panels: distribution of the values of the microphysical parameters ϵ_e , ϵ_B , homogeneous density n_0 and electron slope p . Bottom four panels: distribution of the isotropically equivalent initial kinetic energy E_0 , bulk Lorentz factor Γ_0 , break frequency ν_b and optical spectral index for the late prompt emission β_0 . The hatched areas correspond to the distribution of parameters found by Panaitescu & Kumar (2002) fitting the afterglow of 10 pre-Swift bursts. They are shown for comparison.

bursts with measured E_{peak} , the peak energy of the νF_ν spectrum of the proper prompt emission. We found no contradictory cases (i.e. an observed jet break occurring in a late prompt-dominated GRB), except for GRB 060614.

There are some additional bursts for which the presence of a jet break has been claimed in the literature. For instance, in GRB 050319, Cusumano et al. (2006) suggest that the break in the X-ray light curve at 27 000 s (observed time) could be a jet break, but also discuss the problems with this interpretation due to the unusual pre- and post-break slopes. In our scheme, the observed break simply corresponds to T_A .

For GRB 050730, Pandey et al. (2006) consider the change of slopes at ~ 0.1 d (observed time) in the optical light curve as indicative of a jet break. In our interpretation, instead, the change of

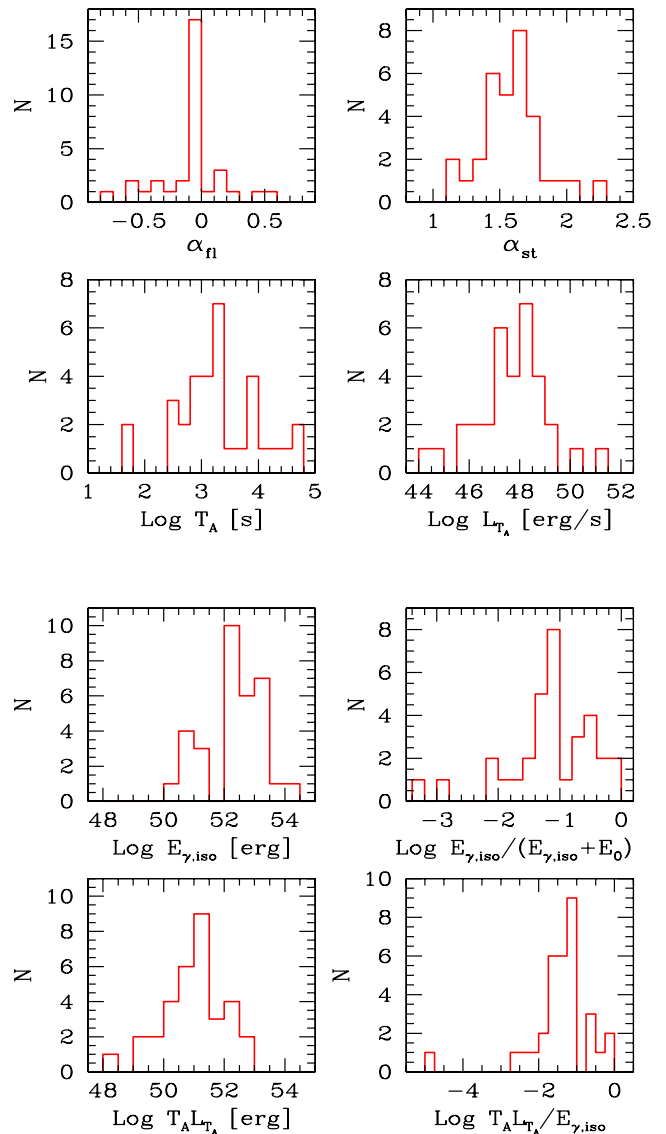


Figure 11. Top four panels: distributions of the decay indices of the late prompt emission, α_{fl} and α_{st} , of T_A and of the 0.3–10 keV luminosity at the time T_A . Bottom four panels: distributions of the isotropic energy $E_{\gamma,iso}$ of the early prompt radiation, of the ratio $E_{\gamma,iso}/(E_{\gamma,iso} + E_0)$, which provides an estimate of the efficiency of the prompt emission; of the energy $T_A L_{T_A}$, and of the ratio $T_A L_{T_A}/E_{\gamma,iso}$.

the flux decay slope is due to the late prompt emission providing a relevant contribution after $\sim 3 \times 10^3$ (rest-frame time).

Malesani et al. (2007) claim the presence of a possible jet break in the optical light curve of GRB 070110 at ~ 5 d (observed time). According to our findings, this can indeed be a jet break that should also be visible in X-rays.

In the light curves examined here, there are also a few examples of slope changes that could be jet breaks, but for which we could not find any report in the literature. The optical light curve of GRB 060206 may be one of such cases (see the last optical point in Fig. 4). For this GRB, the presence of the jet break is expected only in the optical, since the X-rays are dominated by the late prompt component. Note that the corresponding t_j would make this burst consistent with the Ghirlanda relation (see the vertical grey line in Fig. 4). Another example is visible in the X-ray flux decay of GRB

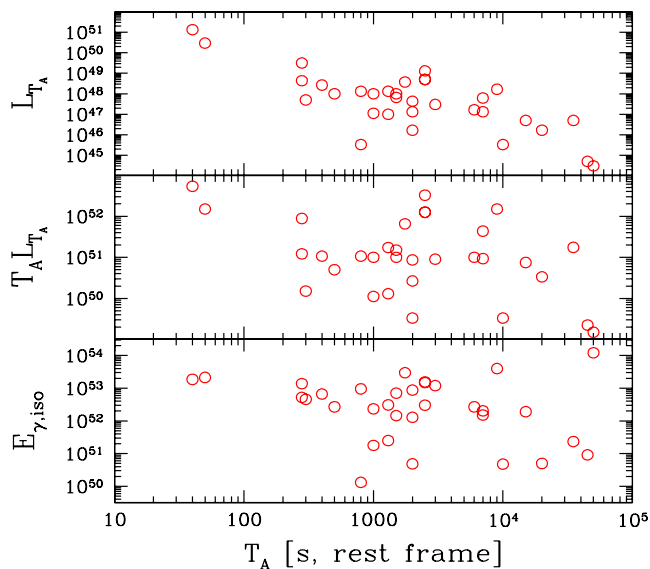


Figure 12. The luminosity of the late prompt emission L_{T_A} (in erg s^{-1}) at T_A , the corresponding energy $T_A L_{T_A}$ (in erg) and the isotropic energy $E_{\gamma, \text{iso}}$ (in erg) as functions of T_A . Note that L_{T_A} anticorrelates with T_A , in such a way that the energy $T_A L_{T_A}$ has a relatively narrow distribution (see also the corresponding histogram in Fig. 11).

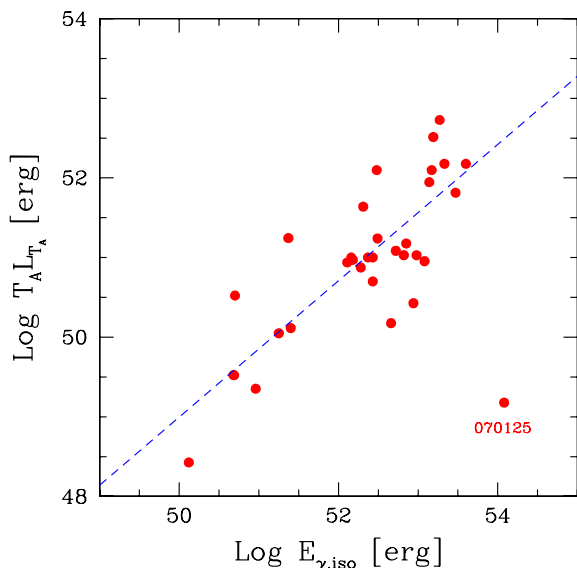


Figure 13. Energy of the late prompt emission, estimated as $T_A L_{T_A}$, as a function of the isotropic energy of the prompt emission, $E_{\gamma, \text{iso}}$. The dashed line corresponds to the least-square fit, $[T_A L_{T_A}] \propto E_{\gamma, \text{iso}}^{0.86}$ (chance probability $P = 2 \times 10^{-7}$, excluding the outlier GRB 070125).

061121, at $\sim 10^5$ s (rest frame, see Fig. 7). Unfortunately, there are no optical data at this late time to confirm it. Again, if this is a jet break, the burst would be consistent with the Ghirlanda relation (see the vertical grey line in Fig. 7). Also in GRB 071010, there could be a jet break in optical, after $\sim 10^5$ s (rest frame, see Fig. 8) but its interpretation is difficult because of an optical/X-ray flare occurring just before. Finally, for GRB 080310, a steepening of the optical light curve after $\sim 10^5$ s (rest frame, see Fig. 9) could be a jet break, as also supported by a steepening in the X-ray light curve, i.e. (marginally) dominated by the afterglow component.

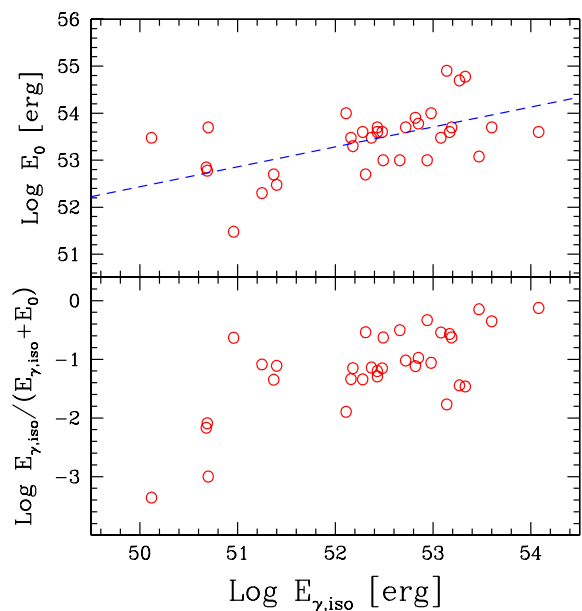


Figure 14. Top panel: the kinetic energy E_0 after the prompt emission as a function of $E_{\gamma, \text{iso}}$. The dashed line is a least-square fit, yielding $E_0 \propto E_{\gamma, \text{iso}}^{0.42}$ (chance probability $P \sim 10^{-3}$, excluding GRB 070125). Bottom panel: the efficiency of the prompt emission estimated as $E_{\gamma, \text{iso}} / (E_{\gamma, \text{iso}} + E_0)$ as a function of $E_{\gamma, \text{iso}}$. There seems to be weak correlation, in the sense that weaker bursts would have the smaller efficiency. See the corresponding distribution in Fig. 11. Here and in the other figures, the plotted values of $E_{\gamma, \text{iso}}$ are neither bolometric nor K -corrected, but refer to the observed 15–150 keV range.

We plan to discuss in more detail these possible jet breaks in a forthcoming paper (Nardini et al., in preparation).

4.3 Prompt and afterglow energetics

As the X-ray luminosity L_X is found to be often dominated by the late prompt emission, *it does not provide a proxy for the afterglow bolometric luminosity*. Since L_X exceeds what observed in the other spectral bands, the estimated luminosities and total energetics produced by the afterglow are radically smaller than what simply inferred from L_X .

This exacerbates the problem of understanding why the early prompt emission is larger than the afterglow one, if the former is dissipated in internal shocks. In fact, while in external shocks, believed to be responsible for the afterglow, a fraction of the whole fireball kinetic energy is available, in internal shocks only a fraction of the *relative* kinetic energy between two colliding shells can be dissipated as radiation. If such fractions are similar, the ‘bolometric afterglow fluence’ is expected to be a factor of ~ 10 larger than the bolometric early prompt fluence. The opposite is observed, and the discrepancy is more extreme if L_X provides only an upper limit to the afterglow contribution, as in our interpretation.

Bearing in mind that it is often dangerous to claim correlations between luminosities or energetics, since both quantities are function of redshift, we can compare Fig. 13 with Fig. 14. It can be seen that the correlation between the late prompt energetics measured by $T_A L_{T_A}$ and $E_{\gamma, \text{iso}}$ is stronger than the correlation between the kinetic energy (after the early prompt) E_0 and $E_{\gamma, \text{iso}}$. A least-square fit yields $(T_A L_{T_A}) \propto E_{\gamma, \text{iso}}^{0.86}$ (chance probability $P = 2 \times 10^{-7}$) and $E_0 \propto E_{\gamma, \text{iso}}^{0.42}$ (chance probability $P \sim 10^{-3}$). If the $T_A L_{T_A} - E_{\gamma, \text{iso}}$ relation

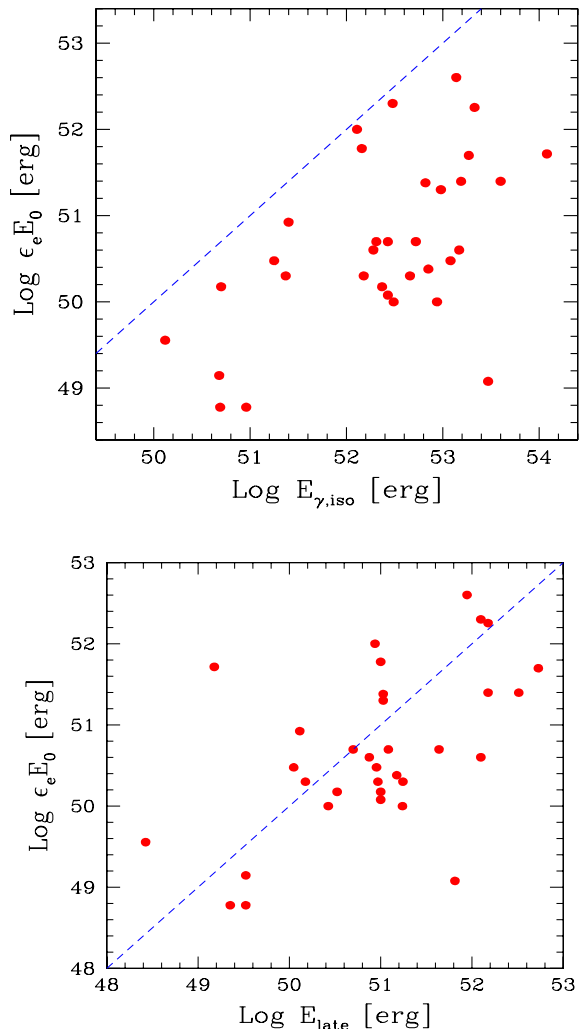


Figure 15. The energetics of the afterglow component, estimated as $\epsilon_e E_0$, as a function of: (top panel) $E_{\gamma,iso}$, the energetics of the prompt emission as measured in the 15–150 keV band (rest frame) – the dashed line corresponds to equal values; (bottom panel) E_{late} , the energetics of the late prompt emission, as measured in the (rest frame) 0.3–10 keV band and approximated by $T_A L_{T_A}$.

is not a mere product of the common redshift dependence (which, however, should also affect the E_0 – $E_{\gamma,iso}$ relation), this suggests that the early and late prompt phases of emission are related.

In Fig. 15 (top panel), $\epsilon_e E_0$ (which can be considered as an upper limit to the bolometric afterglow luminosity) is compared to $E_{\gamma,iso}$, the energetic of the prompt emission as measured in the 15–150 keV band (rest frame). $E_{\gamma,iso}$ exceeds the afterglow energetics by almost two orders of magnitudes. In the bottom panel of the same figure, $\epsilon_e E_0$ is plotted against the energetics of the late prompt emission E_{late} , approximated by the quantity $T_A L_{T_A}$. These quantities do not correlate, suggesting that they are two separated components.

To summarize: all indications gathered from the analysis of the energetics suggest that what we have called ‘late prompt emission’ is a phenomenon not related to the afterglow, but it is more connected to the same engine producing the early prompt. Furthermore, the energetics associated to the afterglow emission is on average a small fraction of the total energy of the burst.

5 DISCUSSION AND CONCLUSIONS

The proposed scheme appears to be suitable to account for the diversity of the optical and X-ray light curves of GRBs, at the expense of introducing, besides the standard afterglow emission resulting from the external (forward) shock, another component. This has been simply parametrized with seven free parameters. The distributions of these parameters are not particularly clustered around mean values, except for the time decay slopes α_{fl} and α_{st} (see below). However, this should not be taken as a potential problem for the proposed idea, since even the well-established afterglow model, when applied to the optical and X-ray afterglows of pre-Swift GRBs, yield broad parameter distributions (see Fig. 10 and Panaitescu & Kumar 2002).

Our phenomenological approach should be considered as a first step towards the construction of a convincing physical model. As discussed in the introduction, there has been already a blooming of theoretical ideas, but a general consensus has not yet been reached. Our findings can shed some light and help to discriminate among the different proposals.

As an illustrative example, the proposed scenario can be contrasted with the alternative idea that GRBs are characterized by two jets with different opening angles (see the introduction). In the latter interpretation, if the line of sight lies within the wide cone but outside the narrow one, the emission from the narrow jet will be observable when Γ has decreased to $\Gamma \sim 1/\theta_v$, and the corresponding afterglow light curve can reproduce the flat-steep-flat behaviour and present a break (at T_A). However, it is hard to explain why the flat-steep-flat trend is not observed in the optical, as in a (narrow jet) afterglow the optical and X-ray fluxes should temporally track each other. The ‘late prompt’ scenario appears to provide a better interpretation of the data.

Within the proposed scheme, some light can be shed on the puzzling issue about jet breaks.

They can be achromatic if the afterglow component is observed in different bands. These may not be the case for several bursts. Furthermore, there are a few in which the late prompt emission, dominating both the optical and X-ray flux, hides jet breaks at all times. For these bursts, a break at the time T_A is visible in both the X-ray and optical bands, and it can be erroneously be taken as a jet break, since it is achromatic. Only a densely sampled light curve in both bands can help to discriminate the presence of a real jet break. Note that the bursts in our sample, selected for having an estimate of extinction in the host, are better sampled optically than the rest of the bursts, for which it would be difficult to reliably estimate the relative importance of the two components.

Another relevant consequence of our scenario is that, even when a jet break is observed, the after-break light curve can be flatter than predicted, since the late prompt flux can contribute after t_j . This implies that the so-called closure relations, linking the flux decay slopes before and after the break with the spectral index, should be taken with care. In this respect, it is worth stressing that the closure relations, and in general the simplified afterglow scenario predicting them, treat the microphysical parameters ϵ_e and ϵ_B as constants in time. We adopt the same simplification, but this might become a crucial issue once we will have a convincing physical interpretation predicting their time behaviour.

From our modelling, the steep decay of the late prompt emission can be described by a power law with slope $\alpha_{st} \sim 1.6$. This is intriguingly similar to the time dependence of the mass accretion rate during the fall-back phase, and to the average decay of the X-ray flare luminosity, as analysed by Lazzati et al. (2008). This is

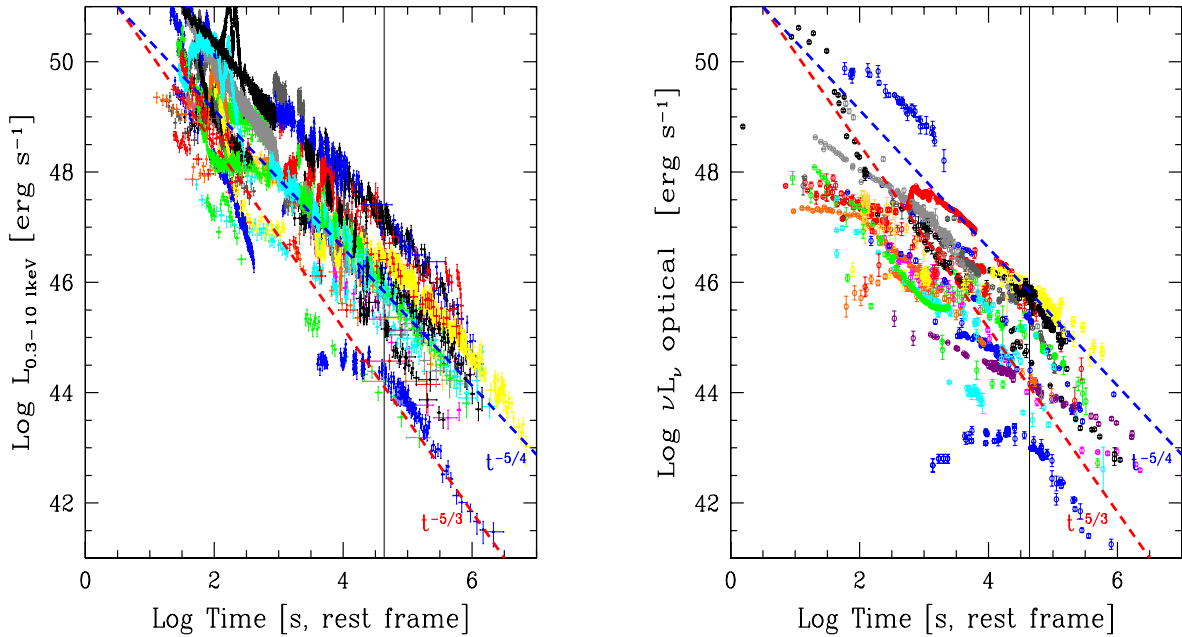


Figure 16. The light curves of all the 33 GRBs in the X-rays (left-hand panel) and optical (right-hand panel). For comparison, the dashed lines correspond to $t^{-5/4}$ and $t^{-5/3}$, as labelled. Especially in the X-rays, the luminosity profile seems to be flatter than $t^{5/3}$ and closer to a $t^{-5/4}$ decay. However, this behaviour is due to the contribution in some GRBs of the afterglow emission at late times, flattening the overall light curve. See Fig. 17 for comparison.

not the average decay slope observed: the X-ray and optical light curves are flatter than $L(t) \propto t^{-5/3}$ (see Fig. 16), but this is due to the contribution, especially at early and late times, and in the X-rays, of the afterglow contribution. Fig. 17 shows the results of our light curve modelling for the optical and X-rays bands. The late prompt light curves are indeed steeper, on average, than the sum of the two components that reproduce the data. We consider this as a main result of our analysis, because it suggests that the late prompt emission can be interpreted as due to the late time accretion on to a black hole of fall-back mass, namely material that failed to reach the escape velocity from the exploding progenitor star, and falls back. According to analytical results (Chevalier 1989) and numerical simulations (e.g. Zhang et al. 2007), the accretion rate decreases in time as $t^{-5/3}$, and can continue for weeks, enough to sustain late prompt emission even at very late times. Our finding also agrees with that obtained by Lazzati et al. (2008) by analysing X-ray flares. They found that the average luminosity of X-ray flares, for a sample of GRBs with known redshift, also decays like $t^{-5/3}$. Such an agreement then suggests that both the X-ray flares and the late prompt emission have a common origin, related to the accretion of the fall-back material. It remains to be explained why this phase is observed after T_A that in some cases can be as long as 10^4 s or more, while the simulations predict a quasi-constant accretion rate for 10^2 – 10^3 s (MacFadyen, Woosley & Heger 2001). There are at least two possibilities. The first one is suggested by the simulations of Zhang et al. (2007) (see their fig. 2) which include the effect of the reverse shock running through the fall-back material. When the reverse shock reaches the inner base, the material is slowed down, and thus the accretion rate is enhanced. The asymptotic $t^{-5/3}$ phase can thus be delayed. The second possibility has been suggested by Ghisellini et al. (2007): even if the total flux produced by the late prompt phase is decaying at the rate $t^{-5/3}$, a decreasing Γ implies that the observed emission comes from an increasing surface ($\propto 1/\Gamma^2$), making the observed decay flatter than $t^{-5/3}$, until, at T_A ,

$\Gamma \sim 1/\theta_j$. After T_A , the whole emitting surface contributes to the detected flux, and the flux decreases as $t^{-5/3}$.

Fig. 17 shows that the sum of the late prompt and afterglow emission makes the optical fluxes to cluster. This occurs because the late prompt emission – though usually not dominant in the optical – narrows the distribution of the optical luminosities at a given time. The vertical dotted line in the figure corresponds to the time (12 h) at which Nardini, Ghisellini & Ghirlanda (2006, 2008), Liang & Zhang (2006) and Kann, Klose & Zeh (2006) found a remarkable clustering of the optical luminosities around two well-separated values. However, the total optical luminosities (right-hand bottom panel of Fig. 17) are more dispersed than the afterglow ones (middle bottom panel).

Our scenario makes some predictions and calls for some consistency checks. We are analysing in more details the data for the GRBs of the present sample to find confirmation of and/or problems with our scenario, and the results will be presented in a forthcoming paper (Nardini et al., in preparation). The main obvious prediction concerns the presence or absence of jet breaks. When both the X-ray and optical light curves are late-prompt dominated, no jet break should be seen. Viceversa, when they both are dominated by the afterglow emission, an achromatic jet break is expected (even if the after-break slope may be shallower). A chromatic jet break should be observed when only one of the two spectral bands is dominated by the afterglow flux. We stress that well-sampled data are required to reliably assess the relative contribution of the two components.

A further general prediction concerns the spectral shape of the late prompt flux. In order for it to be negligible with respect to the afterglow optical emission, there must be a spectral break between the optical and X-ray bands, and the slope below the break should be rather flat. From our modelling, some GRBs require that either this slope is extremely hard or there is a break within the X-ray band (or both). We plan to re-analyse the data of these bursts,

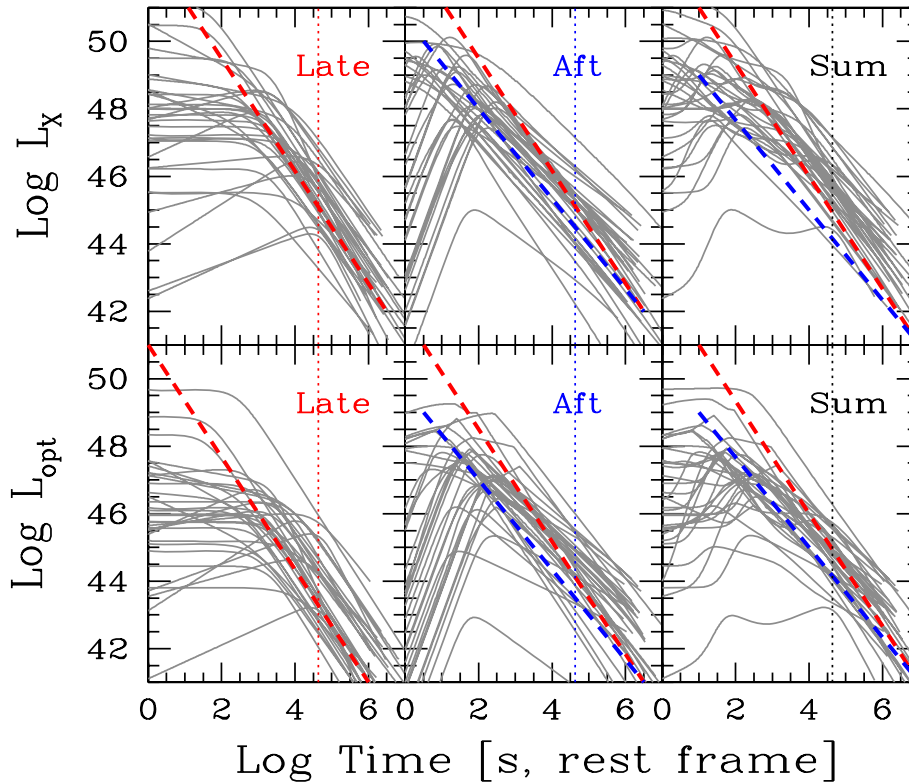


Figure 17. The light curves, as inferred from the modelling, for the 33 GRBs in the X-ray (top panels) and optical (bottom panels) bands. The late prompt (left-hand panels), afterglow (middle panels) and total (left-hand panels) emission are shown. The vertical dotted lines correspond to 12 h. Note that the total optical luminosity at 12 h is more clustered than the late prompt and afterglow luminosities. The dashed lines in the left-hand panels correspond to $L \propto t^{-5/3}$, while in the middle and right-hand panels also decays $L \propto t^{-5/4}$ are shown for reference.

looking for evidence of either a break in the X-ray spectrum, or a very hard optical spectrum (this will depend on the assumed optical extinction). This will impact also on the assumed value of the N_{H} derived by fitting the X-ray data with a simple power-law model.

In our scenario, the observed optical and X-ray fluxes can often be ascribed to different processes. Therefore, when analysing the simultaneous optical to X-ray spectral energy distribution, some caution should be made in interpreting it as a single component connecting the optical and X-ray data. This has to be consistent with the analysis of the entire light curve in both bands, to be confident that they are produced by the same process. Only in such cases, the host galaxy dust extinction can be compared to the X-ray absorption. Spectral information from NIR to ultraviolet would be crucial to this goal.

ACKNOWLEDGMENTS

Financial support was partly provided by a PRIN-INAF 2008 and the ASI I/088/06/0 grants. This work made use of data supplied by the UK Swift Science Data Centre at the University of Leicester.

REFERENCES

- Andreev M., Pozanenko A., 2005, GCN, 4016
 Antonelli L. A., Covino S., Testi V., 2006, GCN, 5546
 Asfandiyarov I., Ibrahimov M., Pozanenko A., 2006, GCN, 5741
 Baliyan K. S., Ganesh S., Vats H. O., Jain J. K., 2006, GCN, 5185
 Beardmore A. P., Osborne J. P., Starling R. L. C., Page K. L., Evans P. A., Cummings J. R., 2008, GCN, 7399
 Berger E., Gladders M., 2006, GCN, 5170
 Berger E., Mulchaey J., 2005, GCN, 3122
 Berger E., Gladders M., Oemler G., 2005, GCN, 3201
 Bhatt B. C., Sahu D. K., 2005, GCN, 3775
 Bloom J. S., Foley R. J., Kocevski D., Perley D., 2006a, GCN, 5217
 Bloom J. S., Perley D., Chen H. W., 2006b, GCN, 5825
 Bloom J. S. et al., 2008, ApJ, submitted (arXiv:0803.3215)
 Blustin A. J. et al., 2006, ApJ, 637, 901
 Burenin R. et al., 2005, GCN, 3718
 Burlon D., Ghirlanda G., Ghisellini G., Lazzati D., Nava L., Nardini M., Celotti A., 2008, ApJ, 685, L19
 Brown P. J., Campana S., Boyd P. T., Marshall F. E., 2006, GCN, 5172
 Butler N. R. et al., 2006, ApJ, 652, 1390
 Campana S., Moretti A., Guidorzi C., Chincarini G., Burrows D. N., 2006a, GCN, 5168
 Campana S. et al., 2006b, GCN, 5163
 Capalbi M. et al., 2007, A&A, 462, 913
 Cenko S. B., 2006a, GCN, 5125
 Cenko S. B., 2006b, GCN, 5844
 Cenko S. B., Baumgartner W. H., 2006, GCN, 5156
 Cenko S. B., Fox D. B., 2006, GCN, 6028
 Cenko S. B., Kulkarni S. R., Gal-Yam A., Berger E., 2005, GCN, 3542
 Cenko S. B. et al., 2006a, ApJ, 652, 490
 Cenko S. B., Berger E., Cohen J., 2006b, GCN, 4592
 Cenko S. B. et al., 2008, ApJ, submitted (arXiv:0808.3983)
 Chandra P., Cenko S. B., Frail D. A., 2008, ApJ, 683, 924
 Chen H. W., Thompson I., Prochaska J. X., Bloom J., 2005, GCN, 3709
 Chen B. A., Lin C. S., Huang K. Y., Ip W. H., Urata Y., 2006, GCN, 4982
 Chen B. A., Huang L. C., Huang K. Y., Urata Y., 2008, GCN, 7395
 Chevalier R. A., 1989, ApJ, 346, 847
 Chiang P. S., Huang K. Y., Ip W. H., Urata Y., Qiu Y., Lou Y. Q., 2005, GCN, 3486
 Chincarini G. et al., 2007, ApJ, 671, 1903
 Cobb B. E., 2006a, GCN, 4972

- Cobb B. E., 2006b, GCN, 5878
Cobb B. E., Baily C. D., 2006, GCN, 5525
Cobb B. E., Baily C. D., van Dokkum P. G., Natarajan P., 2006, ApJ, 651, L85
Covino S., Piranomonte S., Fugazza D., Fiore F., Maleani G., Tagliaferri G., Chincarini G., Stella L., 2005, GCN, 4046
Covino S., Israel G. L., Ghinassi F., Pinilla N., 2006, GCN, 5167
Covino S. et al., 2008a, MNRAS, 388, 347
Covino S., Tagliaferri G., Fugazza D., Chincarini G., 2008b, GCN, 7393
Covino S. et al., 2008c, GCN, 7446
Cucchiara A., Fox D. B., Berger E., 2006, GCN, 4729
Curran P. A. et al., 2007a, MNRAS, 381, L65
Curran P. A. et al., 2007b, A&A, 467, 1049
Cusumano G. et al., 2006, ApJ, 639, 316
Cwiok M. et al., 2008, GCN, 7445
Dado S., Dar A., De Rújula A., 2005, ApJ, 646, L21
D'Elia V. et al., 2005a, GCN, 3746
D'Elia V. et al., 2005b, GCN, 4044
Dai X., Halpern J. P., Morgan N. D., Armstrong E., Mirabal N., Haislip J. B., Reichart D. E., Stanek K. Z., 2007, ApJ, 658, 509
Dainotti M. G., Cardone V. F., Capozziello S., 2008, MNRAS, 391, L79
Della Valle M. et al., 2006a, Nat, 444, 1050
Della Valle M. et al., 2006b, IAUC 8696
De Pasquale M., Cummings J., 2006, GCN, 5130
De Pasquale M. et al., 2006, MNRAS, 365, 1031
De Pasquale M. et al., 2007, MNRAS, 377, 1638
de Ugarte Postigo A. et al., 2007, A&A, 462, L57
Durig D. T., Price T., 2005, GCN, 4023
Efimov Y., Romyantsev V., Pozanenko A., 2006a, GCN, 5850
Efimov Y., Romyantsev V., Pozanenko A., 2006b, GCN, 5870
Eichler D., Granot J., 2006, ApJ, 641, L5
Ellison S. L. et al., 2006, MNRAS, 372, L38
Evans P. A., Beardmore A. P., Godet O., Page K. L., 2006, GCN, 5554
Evans P. A. et al., 2007, A&A, 469, 379
Falcone A. D., Burrows D. N., Morris D., Racusin J., O'Brien P. T., Osborne J. P., Gehrels N., 2006, GCN, 5009
Foley R. J., Chen H. W., Bloom J., Prochaska J. X., 2005, GCN, 3483
Foley R. J. et al., 2006, ApJ, 645, 450
Fox D. B., Berger E., Price P. A., Cenko S. B., 2007, GCN, 6071
French J., Jelinek M., 2006, GCN, 5165
French J., Melady G., Hanlon L., Jelinek M., 2006, GCN, 5257
Fugazza D., D'Avanzo P., Malesani D., 2006, GCN, 5513
Fynbo J. P. U., Hjorth J., Jensen B. L., Jakobsson P., Moller P., Näränen J., 2005a, GCN, 3136
Fynbo J. P. U. et al., 2005b, GCN, 3176
Fynbo J. P. U., Jensen B. L., Hjorth J., Woller K. G., Watson D., Fouque P., Andersen M. I., 2005c, GCN, 3736
Fynbo J. P. U. et al., 2005d, GCN, 3749
Fynbo J. P. U. et al., 2005e, GCN, 3756
Fynbo J. P. U. et al., 2005f, GCN, 3874
Fynbo J. P. U., Limousin M., Castro Cerón J. M., Jensen B. L., Näränen J., 2006a, GCN, 4692
Fynbo J. P. U. et al., 2006b, Nat, 444, 1047
Fynbo J. P. U. et al., 2006c, GCN, 5651
Gal-Yam A., Fox D. B., Price P. A., 2006, Nat, 444, 1053
Garnavich P., Prieto J. L., Pogge R., 2008a, GCN, 7409
Garnavich P., Prieto J. L., Pogge R., 2008b, GCN, 7414
Genet F., Daigne F., Mochkovitch R., 2007, MNRAS, 381, 732
Ghirlanda G., Ghisellini G., Lazzati D., 2004, ApJ, 616, 331
Ghirlanda G., Nava L., Ghisellini G., Firmani C., 2007, A&A, 466, 127
Ghisellini G., Ghirlanda G., Nava L., Firmani C., 2007, ApJ, 658, L75
Gomboc A. et al., 2008, ApJ, 687, 443
Greco G. et al., 2006, GCN, 5526
Greco G. et al., 2007, GCN, 6047
Grupe D. et al., 2006, GCN, 5517
Grupe D. et al., 2007, ApJ, 662, 443
Guidorzi C. et al., 2006, GCN, 5633
Guidorzi C., Gomboc A., Kobayashi S., 2007, A&A, 463, 539
Hafizov B., Sharapov D., Pozanenko A., Ibrahimov M., 2006, GCN, 4990
Haislip J. et al., 2005, GCN, 3568
Halpern J. P., Armstrong E., 2006a, GCN, 5851
Halpern J. P., Armstrong E., 2006b, GCN, 5853
Halpern J. P., Mirabal N., Armstrong E., 2006, GCN, 5840
Halpern J. P., Mirabal N., Armstrong E., 2006, GCN, 5847
Hill G., Prochaska J. X., Fox D., Schaefer B., Reed M., 2005, GCN, 4255
Hill J., Ragazzoni R., Baruffolo A., Garnavich P., 2008, GCN, 7523
Henyeh T., Kocka M., Hroch F., Jelinek M., Hudec R., 2005, GCN, 4026
Holman M., Garnavich P., Stanek K. Z., 2005, GCN, 3716
Holland S. T. et al., 2007, AJ, 133, 122
Homewood A., Hartmann D. A., Garimella K., Henson G., McLaughlin J., Brimeyer A., 2005, GCN, 3491
Huang K. Y., Ip W. H., Lee Y. S., Urata Y., 2006, GCN, 5549
Huang K. Y. et al., 2007, ApJ, 654, L25
Ioka K., Toma K., Yamazaki R., Nakamura T., 2006, A&A, 458, 7
Jakobsson P., Fynbo J. P. U., Paraficz D., Telting J., Jensen B. L., Hjorth J., Castro Cerón J. M., 2005a, GCN, 4029
Jakobsson P., Paraficz D., Telting J., Fynbo J. P. U., Jensen B. L., Hjorth J., Castro Cerón J. M., 2005b, GCN, 4015
Jaunsen A. O., Malesani D., Fynbo J. P. U., Sollerman J., Vreeswijk P. M., 2007, GCN, 6010
Jelínek M., Kubánek P., Prouza M., 2006, GCN, 4976
Jelínek M., Castro-Tirado A. J., Chantry V., Plá J., 2008, GCN, 7476
Kamble A., Resmi L., Misra K., 2007, ApJ, 664, L5
Kamble A., Misra K., Bhattacharya D., Sagar R., 2008, MNRAS, submitted (arXiv:0806.4270)
Kann D. A., Hoegner C., 2006, GCN, 5182
Kann D. A., Klose S., Zeh A., 2006, ApJ, 641, 993
Kann D. A. et al., 2008, ApJ, submitted (arXiv:0712.2186)
Kannappan S., Garnavich P., Stanek K. Z., Christlein D., Zaritsky D., 2005, GCN, 3778
Karimov R., Hafizov B., Pozanenko A., Ibrahimov M., 2006, GCN, 5112
Kennea J. A., Burrows D. N., Goad M., Norris J., Gehrels N., 2005, GCN, 4022
Khamitov I. et al., 2006a, GCN, 5173
Khamitov I. et al., 2006b, GCN, 5177
Khamitov I. et al., 2006c, GCN, 5183
Khamitov I. et al., 2006d, GCN, 5186
Khamitov I. et al., 2006e, GCN, 5189
Khamitov I. et al., 2006f, GCN, 5193
Kinugasa K., 2008, GCN, 7413
Klotz A., Böer M., Atteia J. L., Stratta G., Behrend R., Malacrino F., Damerdjy Y., 2005a, A&A, 439, L35
Klotz A., Böer M., Atteia J. L., 2005b, GCN, 3720
Klotz A. et al., 2008, A&A, 483, 847
Koppelman M., 2006, GCN, 4977
Krugly Y., Slyusarev I., Pozanenko A., 2008, GCN, 7519
Lazzati D., Perna R., 2007, MNRAS, 375, L46
Lazzati D., Perna R., Begelman M. C., 2008, MNRAS, 388, L15
Li W., Jha S., Filippenko A. V., Bloom J. S., Pooley D., Foley R. J., Perley D. A., 2005, GCN, 4095
Li W., Bloom J. S., Chornock R., Foley R. J., Perley D. A., Filippenko A. V., 2008a, GCN, 7430
Li W., Chornock R., Perley D. A., Filippenko A. V., 2008b, GCN, 7438
Liang E., Zhang B., 2006, ApJ, 638, 67
Lin C. S., Huang K. Y., Ip W. H., Urata Y., 2006, GCN, 5169
MacFadyen A. I., Woosley S. E., Heger A., 2001, ApJ, 550, 410
Mangano V. et al., 2007a, ApJ, 654, 403
Mangano V. et al., 2007b, A&A, 470, 105
Malesani D., Piranomonte D., Fiore F., Tagliaferri G., Fugazza D., Cosentino R., 2005, GCN, 3469
Malesani D., Fynbo J. P. U., Jaunsen A. O., Vreeswijk P. M., 2007, GCN, 6021
Marshall F. E., Holland S. T., Page K. L., 2006, GCN, 5833
Mason K. O. et al., 2006, ApJ, 639, 311

- Melandri A. et al., 2006a, GCN, 4968
Melandri A. et al., 2006b, GCN, 5827
Mescheryakov A., Burenin R., Pavlinsky M. et al., 2006, GCN, 5524
Milne P. A., 2006, GCN, 5127
Milne P. A., Williams G. G., 2008a, GCN, 7387
Milne P. A., Williams G. G., 2008b, GCN, 7432
Mirabal N., Bonfield D., Schawinski K., 2005, GCN, 3488
Mirabal N., Halpern J., Thorstensen J. R., 2007, GCN, 6096
Misra K., Bhattacharya D., Sahu D. K., Sagar R., Anupama G. C., Castro-Tirado A. J., Guziy S. S., Bhatt B. C., 2007, A&A, 464, 903
Molinari E. et al., 2007, A&A, 469, L13
Monard B., 2005, GCN, 3728
Morgan N. D., Dai X., 2006, GCN, 5175
Morgan N. D., Vanden Berk D. E., Brown P., Evans P. A., 2006, 5553
Morris D., Burrows D., Gehrels N., Greiner J., Hinshaw D., 2006, GCN, 4694
Mundell C. G., Steele I. A., 2006, GCN, 5119
Mundell C. G. et al., 2007, ApJ, 660, 489
Nardini M., Ghisellini G., Ghirlanda G., 2006, A&A, 451, 821
Nardini M., Ghisellini G., Ghirlanda G., 2008, MNRAS, 386, L87
Norris J. et al., 2005, GCN, 4013
Nousek J. A. et al., 2005, ApJ, 642, 389
Novak R., 2005, GCN, 4027
Novak R., 2008, GCN, 4504
Nysewander M., Reichart D., Ivarsen K., Foster A., LaCluyze A., Crain J. A., 2006, GCN, 5545
Oates S. R., Grupe D., 2006, GCN, 5519
Oates S. R. et al., 2007, MNRAS, 380, 270
Osip D., Chen H. W., Prochaska J. X., 2006, GCN, 5715
Page K. L., Beardmore A. P., Goad M. R., Kennea J. A., Burrows D. N., Marshall F. Smale A., 2005, GCN, 3837
Page K. L. et al., 2006, GCN, 5823
Page K. L. et al., 2007, ApJ, 663, 1125
Panaitescu A., 2007a, MNRAS, 380, 374
Panaitescu A., 2007b, MNRAS, 379, 331
Panaitescu A., 2008, MNRAS, 383, 1143
Panaitescu A., Kumar P., 2000, ApJ, 543, 66
Panaitescu A., Kumar P., 2001a, ApJ, 554, 667
Panaitescu A., Kumar P., 2001b, ApJ, 560, L49
Panaitescu A., Kumar P., 2002, ApJ, 571, 779
Panaitescu A., Mészáros P., Burrows D., Nousek J., Gehrels N., O'Brien P., Willingale R., 2006, MNRAS, 369, 2059
Pandey S. B. et al., 2006, A&A, 460, 415
Pavlenko E., Efimov Y., Shlyapnikov A., Baklanov A., Pozanenko A. Ibrahimov M., 2005, GCN, 3744
Pe'er A., Mészáros P., Rees M. J., 2006, ApJ, 652, 482
Perley D. A., Bloom J. S., 2008a, GCN, 7406
Perley D. A., Bloom J. S., 2008b, GCN, 7535
Perley D. A., Chornock R., Bloom J. S., Fassnacht C., Auger M. W., 2007, GCN, 6850
Perley D. A. et al., 2008a, ApJ, 672, 449
Perley D. A. et al., 2008b, ApJ, 688, 270
Perri M. et al., 2005, A&A, 442, L1
Perri M. et al., 2007, A&A, 471, 83
Piranomonte S. et al., 2005, GCN, 4032
Price P. A., Berger E., Fox D. B., 2006, GCN, 5275
Prochaska J. X., Bloom J. S., Wright J. T., Butler R. P., Chen H. W., Vogt S. S., Marcy G. W., 2005, GCN, 3833
Prochaska J. X., Chen H. W., Bloom J. S., Falco E., Dupree A. K., 2006, GCN, 5002
Prochaska J. X., Perley D. A., Modjaz M., Bloom J. S., Poznanski D., Chen H.-W., 2007, GCN, 6864
Prochaska J. X., Murphy M., Malec A. L., Miller K., 2008, GCN, 7388
Quimby R. M. et al., 2006, ApJ, 640, 402
Racusin J. L. et al., 2008, Nat, 455, 183
Rol E., Jakobsson P., Tanvir N., Levan A., 2006, GCN, 5555
Romano P. et al., 2006, A&A, 456, 917
Ruffini R. et al., 2008, Proc. XI Marcel Grossmann Meeting, in press (arXiv:0804.2837)
Ruiz-Velasco A. E. et al., 2007, ApJ, 669, 1
Rumyantsev V., Pozanenko A., 2006, GCN, 5181
Rumyantsev V., Pozanenko A., Ibrahimov M., Asfandyarov I., 2006, GCN, 5306
Rykoff E. S. et al., 2005, ApJ, 631, L121
Rykoff E. S. et al., 2006, ApJ, 638, L5
Schady P. et al., 2007, MNRAS, 377, 284
Schlegel D. J., Finkbeiner D. P., Davis M., 1998, ApJ, 500, 525
Schmidt B., Peterson B., Lewis K., 2006, GCN, 5258
Shao L., Dai Z. G., 2007, ApJ, 660, 1319
Shao L., Dai Z. G., Mirabal N., 2008, ApJ, 675, 507
Sharapov D., Djupvik A., Pozanenko A., 2006, GCN, 5267
Skvare J., 2006, GCN, 5511
Soderberg A. M. et al., 2007, ApJ, 661, 982
Sollerman J. et al., 2007, A&A, 466, 839
Sota A., Castro-Tirado A. J., Guziy S., Jelínek M., de Ugarte Postigo A., Gorosabel J., Bodganov A., Pérez-Ramírez M. D., 2005, GCN, 3705
Soyano T., Mito H., Urata Y., 2006, GCN, 5548
Stanek K. Z. et al., 2007, ApJ, 654, L21
Still M. et al., 2005, ApJ, 635, 1187
Swan H., Yuan F., Rujopakarn W., 2008, GCN, 7470
Tagliaferri G. et al., 2005, Nat, 436, 985
Tanvir N. R., Perley D. A., Levan A. J., Bloom J. S., Fruchter A. S., Rol E., 2008, GCN, 7621
Terra F. et al., 2006, GCN, 5192
Terra F. et al., 2007, GCN, 6064
Thöne C. C. et al., 2006, GCN, 5373
Thöne C. C. et al., 2008, A&A, submitted (arXiv:0806.1182)
Toma K., Ioka K., Yamazaki R., Nakamura T., 2006, ApJ, 640, L139
Torii K., 2006a, GCN, 5642
Torii K., 2006b, GCN, 5845
Torii K., BenDaniel M., 2005, GCN, 3470
Troja E. et al., 2007, ApJ, 665, L97
Uemura M., Arai A., Uehara T., 2006, GCN, 5828
Uemura M., Arai A., Uehara T., 2007, GCN, 6039
Uhm L. Z., Beloborodov A. M., 2007, ApJ, 665, L93
Updike A. C. et al., 2008, ApJ, in press (arXiv:0805.1094)
Urata Y., Chen T. W., Huang K. Y., Huang K. Y., Im M., Lee I., 2008a, GCN, 7415
Urata Y., Im M., Lee I., Huang K. Y., Zheng W. K., Xin L. P., 2008b, GCN, 7435
Vreeswijk P. M., Smette A., Malesani D., Fynbo J. P. U., Jensen B. M., Jakobsson P., Jaunsen A. O., Ledoux C., 2008, GCN, 7444
Watson D. et al., 2006, ApJ, 652, 1011
Wegner G., Garnavich P., Prieto J. L., Stanek K. Z., 2008, GCN, 7423
Willingale R. et al., 2007, ApJ, 662, 1093
Woźniak P. R., Vestrand W. T., Wren J. A., White R. R., Evans S. M., Caspersen D., 2005, ApJ, 627, L13
Woźniak P. R., Vestrand W. T., Wren J. A., White R. R., Evans S. M., Caspersen D., 2006, ApJ, 642, L99
Woźniak P. R., Vestrand W. T., Wren J. A., Davis H., 2008, GCN, 7464
Xing L. P., Zhai M., Qiu Y. L., Wei J. Y., Hu J. Y., Deng J. S., Urata Y., Zheng W. K., 2007, GCN, 6035
Yoshida M., Yanagisawa K., Kawai N., 2007, GCN 6050
Yoshida M., Yanagisawa K., Shimizu Y., Nagayama S., Toda H., Kawai N., 2008, GCN, 7410
Yost S. A. et al., 2007, ApJ, 168, 925
Zhang B., 2007, Adv. Space Res., 40, 1186
Zhang B., Mészáros P., 2001, ApJ, 552, L35
Zhang B. et al., 2006, ApJ, 642, 354
Zhang W., Woosley S. E., Heger A., 2007, ApJ, 679, 639

APPENDIX A: PHOMETRIC DATA REFERENCES

References of the photometric data plotted in Figs 1–9 and 16.

- GRB 050318: Still et al. (2005).
- GRB 050319: Woźniak et al. (2005), Mason et al. (2006), Quimby et al. (2006), Huang et al. (2007) and Kamble, Resmi & Misra (2007).
- GRB 050401: Rykoff et al. (2005), De Pasquale et al. (2005), Watson et al. (2006) and Kamble et al. (2008).
- GRB 050408: Foley et al. (2006) and de Ugarte Postigo et al. (2007).
- GRB 050416a: Holland et al. (2007) and Soderberg et al. (2007).
- GRB 050525a: Torii & BenDaniel (2005), Malesani et al. (2005), Chiang et al. (2005), Mirabal, Bonfield & Schawinski (2005), Homewood et al. (2005), Haislip et al. (2005), Della Valle et al. (2006b), Klotz et al. (2005a) and Blustin et al. (2006).
- GRB 050730: Sota et al. (2005), Holman, Garnavich & Stanek (2005), Burenin et al. (2005), Klotz et al. (2005b), D’Elia et al. (2005a), Bhatt & Sahu (2005), Kannappan et al. (2005) and Pandey et al. (2006).
- GRB 050801: Monard (2005), Fynbo et al. (2005c) and Rykoff et al. (2006).
- GRB 050802: Pavlenko et al. (2005), Fynbo et al. (2005e) and Oates et al. (2007).
- GRB 050820a: Cenko et al. (2006a).
- GRB 050824: Sollerman et al. (2007).
- GRB 050922c: Norris et al. (2005), Jakobsson et al. (2005b), Andreev & Pozanenko (2005), Durig & Price (2005), Henych et al. (2005), Novak (2005), Piranomonte et al. (2005), D’Elia et al. (2005b), Covino et al. (2005) and Li et al. (2005).
- GRB 051111: Butler et al. (2006) and Yost et al. (2007).
- GRB 060124: Romano et al. (2006) and Misra et al. (2007).
- GRB 060206: Woźniak et al. (2006), Stanek et al. (2007) and Curran et al. (2007a).
- GRB 060210: Stanek et al. (2007), Curran et al. (2007b) and Cenko et al. (2008).
- GRB 060418: Melandri et al. (2006a), Cobb (2006a), Jelínek, Kubánek & Prouza (2006), Koppelman (2006), Chen et al. (2006), Hafizov et al. (2006), Karimov et al. (2006) and Molinari et al. (2007).
- GRB 060512: Mundell & Steele (2006), Cenko (2006a), Milne (2006), De Pasquale & Cummings (2006), Cenko & Baumgartner (2006) and Sharapov, Djupvik & Pozanenko (2006).
- GRB 060526: Campana et al. (2006b), French & Jelinek (2006), Covino et al. (2006), Lin et al. (2006), Brown et al. (2006), Khamitov et al. (2006a), Morgan & Dai (2006), Khamitov

- et al. (2006b), Rumyantsev & Pozanenko (2006), Kann & Hoegner (2006), Khamitov et al. (2006c), Baliyan et al. (2006), Khamitov et al. (2006d,e), Terra et al. (2006), Khamitov et al. (2006f), Rumyantsev et al. (2006), Dai et al. (2007) and Thöene et al. (2008).
- GRB 060614: French et al. (2006), Schmidt, Peterson & Lewis (2006), Cobb et al. (2006), Fynbo et al. (2006b), Della Valle et al. (2006), Gal-Yam, Fox & Price (2006) and Mangano et al. (2007b).
- GRB 060729: Grupe et al. (2007).
- GRB 060904b: Skvarc (2006), Oates & Grupe (2006), Mescheryakov et al. (2006), Cobb & Bailyn (2006), Greco et al. (2006), Soyano, Mito & Urata (2006), Huang et al. (2006), Asfandyarov, Ibrahimov & Pozanenko (2006) and Klotz et al. (2008).
- GRB 060908: Nysewander et al. (2006), Antonelli, Covino & Testi (2006), Morgan et al. (2006) and Cenko et al. (2008).
- GRB 060927: Guidorzi et al. (2006), Torii (2006a) and Ruiz-Velasco et al. (2007).
- GRB 061007: Mundell et al. (2007).
- GRB 061121: Page et al. (2006), Melandri et al. (2006b), Uemura, Arai & Uehara (2006), Marshall, Holland & Page (2006), Halpern, Mirabal & Armstrong (2006), Cenko (2006b), Torii (2006b), Halpern, Mirabal & Armstrong (2006), Efimov, Rumyantsev & Pozanenko (2006a), Halpern & Armstrong (2006a,b), Efimov, Rumyantsev & Pozanenko (2006b) and Cobb (2006b).
- GRB 061126: Perley et al. (2008a) and Gomboc et al. (2008).
- GRB 070110: Malesani et al. (2007) and Troja et al. (2007).
- GRB 070125: Cenko & Fox (2006), Xing et al. (2007), Uemura, Arai & Uehara (2007), Greco et al. (2007), Yoshida, Yanagisawa & Kawai (2007), Terra et al. (2007), Mirabal, Halpern & Thorstensen (2007), Updike et al. (2008) and Chandra, Cenko & Frail (2008).
- GRB 071003: Perley et al. (2008b) and Cenko et al. (2008).
- GRB 071003: Covino et al. (2008a) and Cenko et al. (2008).
- GRB 080310: Milne & Williams (2008a), Covino et al. (2008b), Chen et al. (2008), Garnavich, Prieto & Pogge (2008a), Yoshida et al. (2008), Kinugasa (2008), Garnavich, Prieto & Pogge (2008b), Urata et al. (2008a), Wegner et al. (2008), Hill et al. (2008) and Cenko et al. (2008).
- GRB 080319b: Li et al. (2008a), Milne et al. (2008b), Urata et al. (2008b), Li et al. (2008b), Cwiok et al. (2008), Covino et al. (2008c), Woźniak et al. (2008), Swan, Yuan & Rujopakarn (2008), Jelínek et al. (2008), Novak (2008), Krugly, Slyusarev & Pozanenko (2008), Perley & Bloom (2008b), Tanvir et al. (2008) and Bloom et al. (2008).

This paper has been typeset from a $\text{\TeX}/\text{\LaTeX}$ file prepared by the author.